Reviews in Mineralogy & Geochemistry
Vol. 66, pp. 23-52, 2007

Stable Isotope-Based Paleoaltimetry: Theory and Validation

David B. Rowley

Department of the Geophysical Sciences
The University of Chicago
5734 S. Ellis Avenue
Chicago, Illinois, 60637, U.S.A.
rowley@geosci.uchicago.edu

ABSTRACT

Paleoaltimetry is the quantitative estimate of the surface height above mean sea level of ancient landforms. Atmospheric thermodynamic modeling of the behavior of ^{18}O relative to ^{16}O during condensation from water vapor establish the systematic relationship that exists between $\Delta(\delta^{18}O_p)$ and elevation, where $\Delta(\delta^{18}O_p)$ is the difference between a low altitude, preferably sea level $\delta^{18}O_p$ and a potentially high elevation sample. Comparison of model predictions with observations suggests that the model captures the first-order behavior of $\delta^{18}O_p$ during condensation and precipitation in orographic settings. The actual relationship between $\Delta(\delta^{18}O_p)$ and elevation depends sensitively on climate, and specifically starting temperature and to a lesser degree relative humidity. Thermodynamic modeling allows the $\Delta(\delta^{18}O_p)$ and elevation relationship to be explicitly calculated for any given starting climate state. This makes the theoretical approach significantly more appropriate than empirically calibrated approaches based typically on quite limited samples presently available in most orographic settings today.

Paleoaltimetry archives derive their isotopic compositions from surface and or ground water, and hence it is important to understand the systematic differences between these reservoirs and precipitation. Surface waters and ground waters integrate not just the change in isotopic composition with altitude, but also variations in hypsometry within the drainage basin and precipitation amount as functions of elevation. Thus these archives should reflect the precipitation amount weighted hypsometric mean elevation of the (paleo)-drainage basin from which they derive their waters. Analysis of modern data from the Himalayan region supports this expectation. Foreland basin rivers are such integrators and it is shown, using an example from the Siwaliks that the rivers draining the front of the Himalayas in the past had isotopic compositions comparable with modern rivers draining the Himalayan front suggesting little net change in Himalayan hypsometry over the past 11 million years.

INTRODUCTION

Paleoaltimetry is the quantitative estimate of the surface height above mean sea level of features in the past. Unlike quantitative paleobathymetry, which has a long history of development and application, quantitative paleoaltimetry is a recently emerging area of investigation and one still in its infancy of development and validation. Nonetheless, there has been an explosion of interest in paleoaltimetry in the past 10 years and considerable progress since the publication of the benchmark review of this field by Chase et al. (1998). The recent review by Rowley and Garzione (2007) summarizes much of this progress. The focus of the present discussion will be on the theoretical underpinnings of $\delta^{18}O$ isotope-based

1529-6466/07/0066-0002$05.00 DOI: 10.2138/rmg.2007.66.2

approaches to paleoaltimetry and its validation in the modern. Modeling of δ^2H is included for completeness, but is not discussed beyond that. This particular review is not intended to be comprehensive of work in the field of either paleoaltimetry in general or stable isotope paleoaltimetry in particular. Rather the review will address a particular modeling approach to paleoaltimetry, some of the rationale for adopting a theoretical approach as opposed to empirical calibration approaches, and continued validation of this modeling approach using a spectrum of data from the present. In addition, one new application of this approach to the past is outlined exploring paleo-hypsometric relations in paleodrainages feeding the Siwalik foreland basin of the Himalayas. For broader reviews of stable isotope-based paleoaltimetry the reader is directed to Rowley and Garzione (2007), Blisnuik and Stern (2005), as well as important contributions in the present volume, including Quade et al. (2007), Mulch and Chamberlain (2007) and Kohn and Dettman (2007).

The primary foci of paleoaltimetry are regions of the Earth with elevations typically 2 to 3 km and higher. Although these are clearly tectonically interesting and important, it is important to recognize that regions above 2 km represent only about 11% of the surface of the continents and a bit more than 3% of the surface of the Earth as a whole. Much of the interest in paleoaltimetry to date is focused on the Himalayas (Rowley et al. 1999; Garzione et al. 2000a,b; Rowley et al. 2001), Tibetan Plateau (Currie et al. 2005; Cyr et al. 2005; Rowley and Currie 2006) and the Andes (Garzione et al. 2006; Ghosh et al. 2006), regions with current elevations greater than 4 km. Together these represent less than 2% of the surface area of the continents (Fig. 1). Regions such as the Sierra Nevada (Mulch et al. 2006), Cascades (Kohn et al. 2002), western United States (Horton and Chamberlain 2006; Kent-Corson et al. 2006), among other, less highly elevated orographic entities have also been investigated with stable isotope-based paleoaltimetric approaches. It is important to recognize that all such regions represent but a small fraction of the Earth's surface environment.

Paleoaltimetry, at least in its present form, is primarily directed at developing an understanding of the elevation history of what are currently highly elevated regions that represents a small but intriguing fraction of Earth's hypsometric development. It seems clear that as confidence is gained in the ability to discern paleoelevation histories in these

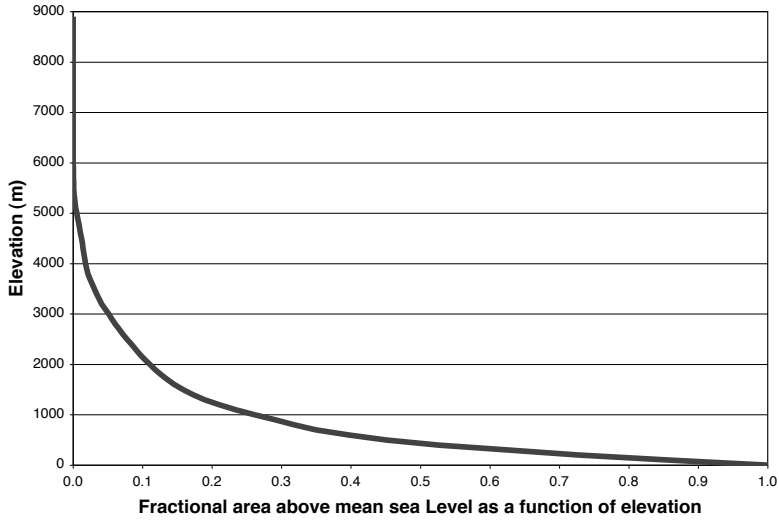

Figure 1. Fractional area of the continents with elevations above mean sea level based on Globe 30 second topography (GLOBE Task Team and others (Hastings 1999).

regions, where the signals are large, there will be increasing interest in the application of these techniques to deeper time and to regions no longer at high elevations.

The majority of continental topography of Earth is, to first order, in simple isostatic equilibrium, and thus there exists a good correlation between topography and crustal thickness. This suggests that estimates of paleoelevation can be derived from dating times of change of crustal thickness as a proxy for elevation. Prior to the ability to independently estimate the elevation of the surface as a function of time, the generally held view was that elevation change was inherently correlated with times of crustal deformation, and in the case of mountain building primarily times of shortening of the crust. The assumption being that if one can date and estimate the magnitude of crustal shortening then the timing and amplitude of surface elevation change can be directly determined, taking appropriate account of isostasy. This obviously does not pertain to regions, such as South Africa where the surface rocks are undeformed, including interbedded marine strata, nor specifically in the cases of rift shoulder uplift, where crustal thickening clearly is not the underlying driver of increases in elevation. However, in orogenic settings this assumption appeared to be an obvious corollary of the process.

Structural analysis of highland areas is, at least in part, motivated to determine the magnitude and timing of shortening from which to derive estimates of the timing of surface uplift. Argand's (1924) insightful surmise of the doubled thickness of Tibetan crust provided considerable impetus to field investigations of the magnitude and timing of crustal deformation as a function of location within the Himalayas and Tibet (see Coward et al. 1988; Dewey et al. 1988) among many other regions. The absence of simple, unequivocal and pervasive evidence of ~50% surface shortening since the late Early Eocene initiation of India-Asia collision (Zhu et al. 2005), in Tibet raises questions regarding this assumption. The relative constancy of elevation of the Tibetan Plateau has been cogently argued to reflect flow in the lower or middle crustal levels in response to potential changes in surface loading (Zhao and Morgan 1987). This point was further emphasized by Royden et al. (1997) in their analysis of eastern Tibet. In eastern Tibet there exist quite clear geologic relations indicating limited Tertiary crustal shortening, and yet modern surface elevations above 4 km argued that relatively recent surface uplift had indeed taken place (Clark et al. 2005). Royden et al (1997) among many others invoke flow of continental crust at lower or mid-crustal depths driven by topographic gradients away from regions of southern and central Tibet elevated earlier in this history.

The potential role of the mantle in the evolution of topography in orogenic settings has been analyzed by Bird (1979), England and Houseman (1986), Molnar et al. (1993) and Garzione et al.(2006) among others. England and Houseman (1986) and Molnar et al. (1993) brought forth arguments, both based on numerical modeling and geological observations that mantle lithospheric thickening and subsequent convective destabilization and removal may have played a significant role in the evolution of Tibetan topography. Pyskylwec et al. (2000) demonstrated that the growth and evolution of Rayleigh-Taylor instabilities in convergence systems depends on a number of parameters, including the rate of convergence, the density field, and the rheology of the mantle lithosphere. These types of instabilities may or may not develop depending on relationships among the various controlling parameters and therefore should not be expected to be an intrinsic contributor in the evolution of every collisional domain.

Both lower or mid-crustal flow and lithospheric mantle contributions decouple surface geology, and particularly evidence of crustal shortening, from elevation history at least in some regions. That is to say that some fraction of the topographic development may not be correlated with or controlled by observable evidence at the surface of crustal thickening. In order to sort out various potential contributions to the elevation history in a given orogenic system it is therefore necessary to have techniques that allow independent estimates of the surface elevation history. One such technique that has been developed that potentially allows for this is stable isotope-based paleoaltimetry. The theoretical basis for this paleoaltimeter has been discussed by Rowley et al. (2001) and Rowley and Garzione (2007) and will be briefly

reviewed and updated here. In order to validate the model, modern data primarily derived from surface waters are discussed with an emphasis on the Himalayas and southern Tibet.

STABLE ISOTOPE-BASED PALEOALTIMETRY

Measurement of $\delta^{18}O$ and $\delta^{2}H$ in precipitation quickly led to the recognition of various factors, often referred to as effects, controlling the spatial variation of isotopic compositions. Among the various effects are temperature, latitude, amount, continentality, and elevation. The relative importance of these various effects has generally been assessed by employing multiple regression techniques to the **g**lobal **n**etwork of **i**sotopes in **p**recipitation (GNIP) datasets (Craig 1961; Dansgaard 1964; Rozanski et al. 1993), a product of the Isotope Hydrology Section of the International Atomic Energy Agency, located in Vienna, Austria (IAEA-Yearly 2004; IAEA-Monthly 2004). The GNIP dataset contains relatively fewer high elevation stations and so the altitude effect is relegated typically to 4th or less significance in controlling the isotopic composition of precipitation (Rozanski et al. 1993). This might be taken to imply stable isotope-based paleoaltimetry has a quite limited potential. However, $\delta^{18}O$ in precipitation exceeding −10 to −15‰ relative to low elevation starting compositions within <100 km in orographic settings are comparable to 75° of the so-called latitudinal effect, thus testifying to the potential significance of elevation in controlling isotopic compositions. More recently, Bowen and Revenaugh (2003) model the spatial pattern of modern isotopic of precipitation using only two parameters the latitude and elevation quite successfully. This approach uses a simple linear scaling of isotopic composition to elevation (Bowen and Revenaugh 2003; Dutton et al. 2005). This approach is quite good at fitting the modern isotopic composition of precipitation but is obviously not applicable to the determination of paleoelevations. In order to investigate the potential for employing oxygen and or hydrogen isotopes as paleoaltimeters, it is important to have a first-order theoretical understanding of why correlation should exist between the isotopic composition of precipitation and elevation. In the following section the theory behind this stable isotope paleoaltimeter is explored, followed by various tests of this model using modern day data.

ATMOSPHERIC THERMODYNAMICS OF OXYGEN AND HYDROGEN ISOTOPE-BASED ESTIMATES OF ELEVATION FROM OROGRAPHIC PRECIPITATION

Rowley et al. (2001) presented a model that theoretically predicts the expected relationship between stable isotopic composition of the condensed water phase and elevation. The model tracks the moist static energy, water vapor content, and water vapor and condensate isotopic composition along ascending, precipitating trajectories and is summarized here. An empirical fit, that is re-examined and updated from Rowley et al. (2001) here, between the condensed phase isotopic composition and precipitation extends the theory such that the output of the model is the expected systematic behavior of oxygen and hydrogen isotopic composition of precipitation as a function of elevation. In this discussion we employ $\Delta(\delta^{18}O)$ as introduced by Ambach et al. (1968) and $\Delta(\delta^{2}H)$, the difference in isotopic composition between a low, preferably near sea level composition and a potentially elevated sample as the monitor of elevation recognizing that this difference rather than the absolute isotopic composition is the measure of elevation. It should be stressed that positive values of $\Delta(\delta^{18}O)$ or $\Delta(\delta^{2}H)$ have no paleoelevation significance, but instead primarily indicate (1) error in the estimate of the mean low altitude isotopic composition used in the normalization, or (2) typical scatter in isotopic data, or (3) significant evaporation of precipitation or surface waters in the unknown site relative to the low elevation normalizing value. Positive values, which if used to estimate

paleoelevation using equations described in this text or comparable ones in Currie et al. (2005) or Rowley and Garzione (2007) yield negative, i.e., below sea level, heights that would in turn imply that the precipitation was enriched beyond its initial values by descending in altitude. This is impossible and hence any such values should simply be ignored in terms of implications for stable isotope-based (paleo)altimetry.

THE MODEL

At equilibrium, there is a fractionation of ^{18}O relative to ^{16}O and ^{2}H relative to ^{1}H that occurs as water vapor condenses to form condensate (water or ice). The magnitude of fractionation, at least according to the model, is determined by the equilibrium fractionation factor, α, that for oxygen is defined as:

$$\alpha_O = \frac{R_p}{R_v} = \frac{\left(\delta^{18}O_p + 1000\right)}{\left(\delta^{18}O_v + 1000\right)}$$

where R_p is the ratio of $^{18}O/^{16}O$ in condensate and R_v is the ratio of $^{18}O/^{16}O$ in water vapor. The quantities $\delta^{18}O_p$, $\delta^{18}O_v$ are the ratios in condensate and vapor, respectively, relative to a standard, (SMOW) expressed as per mil (‰), such that, for oxygen:

$$\delta^{18}O_p = \left(\frac{R_p}{R_{SMOW}} - 1\right) \cdot 1000$$

Substitution of ^{2}H and ^{1}H for ^{18}O and ^{16}O, respectively, in the above results in the identical relations for $^{2}H/^{1}H$ fractionation. The fractionation factor, α, is a function of the temperature at which condensation takes place and the phases involved. In the atmosphere, fractionation occurs between water vapor and liquid water or between water vapor and water ice. The temperature dependence of $\alpha(T)$ has been determined experimentally for liquid-vapor equilibrium (Majoube 1971b; Horita and Wesolowski 1994), and for ice-vapor equilibrium (Merlivat and Nief 1967; Majoube 1971a). Existing experimental results are in quite close agreement and we use these relations in the model (Fig. 2).

Simple application of the empirical fits would imply a greater than 3.4‰ difference between water vapor condensing as liquid water and water ice just above and below 0 °C. However, water is well known to cool below its freezing temperature by 20 K or more and thus we adopt a linear mixing model such that there is not an abrupt step in α_O or α_H at 273.15 K. Thus for temperatures between 273.15 K and 253.15 K we mix between ice and liquid water fractionation (Fig. 2).

At any given T the equilibrium isotopic compositions of oxygen and hydrogen in condensate ($\delta^{18}O_p$ or $\delta^{2}H_p$) and vapor ($\delta^{18}O_v$ or $\delta^{2}H_v$) are described by the relation:

$$\delta^{18}O_p = \alpha_O(T) \cdot \left(\delta^{18}O_v + 1000\right) - 1000$$

and

$$\delta^{2}H_p = \alpha_H(T) \cdot \left(\delta^{2}H_v + 1000\right) - 1000$$

The isotopic composition of the vapor and condensate are simply offset at any given height in the atmosphere by the appropriate equilibrium fractionation factor and hence the derivative of the isotopic composition for the vapor and condensate with respect to elevation are identical as described below by Equation (1). Open system distillation, as modeled by Rayleigh condensation, removes the condensate as it condenses from the vapor leaving the isotopic composition of the residual vapor progressively depleted in ^{18}O and ^{2}H. We use $\zeta = -\ln(p/p_s)$

as our vertical coordinate, where p is ambient pressure and p_s is the surface pressure, such that ζ represents a scale height in the atmosphere. The distillation process can then be expressed by the differential equation:

$$\frac{dR_v}{d\zeta} = \frac{dR_p}{d\zeta} = R_v\left[a(T) - 1\right]\frac{1}{q}\frac{dq}{d\zeta} \tag{1}$$

where R_p and R_v are the isotopic ratios in the incremental condensate and the vapor, respectively, q is the mass mixing ratio of water, and $dq/d\zeta$ is the amount of water condensed from the air parcel in order to maintain saturation as a consequence of adiabatic ascent. From atmospheric thermodynamics it is possible to determine $dq/d\zeta$ with three basic equations. These are:

$$\frac{dz}{d\zeta} = \frac{RT}{g} \tag{2}$$

where z is altitude in meters, and R (without any subscripts) is the gas constant for air (R = 287 J kg^{-1} K^{-1}). The change in temperature with height depends on whether or not condensation is occurring, and for rapidly ascending, thermally isolated parcels is described by the relations

$$\frac{dT}{d\zeta} = -\frac{RT + Lq_s}{C_p + Lq_s\left(\ln(e_s)\right)'} \qquad \text{if moisture is condensing} \tag{3a}$$

$$\frac{dT}{d\zeta} = -\left(\frac{R}{C_p}\right)T \qquad \text{if non-condensing} (q < q_s) \tag{3b}$$

where C_p is the heat capacity of air (1004.0 J kg^{-1} K^{-1}), q_s is the saturation mass mixing ratio of water ($\approx .622\ e_s/p$), e_s is $e_s(T)$, which is the saturation vapor pressure of water as a function of T (Fig. 3), and L is the latent heat contribution due to condensation, which also varies as a function of T. Equation (3b) is the formula for the dry adiabat. Equation (3a) incorporates the change in saturation vapor pressure with temperature through the expression,

$$\left(\ln(e_s)\right)' = \frac{1}{e_s}\frac{de_s}{dT}$$

Finally, the amount of water condensed from the air parcel as ice or liquid in order to maintain saturation is determined through the relation:

$$\frac{1}{q}\frac{dq}{d\zeta} = 1 + \left(\ln(e_s)\right)'\frac{dT}{d\zeta} \qquad \text{if condensing } (q \geq q_s) \tag{4a}$$

$$\frac{1}{q}\frac{dq}{d\zeta} = 0 \qquad \text{if noncondensing} (q < q_s) \tag{4b}$$

If there is no condensation, q is conserved following the air parcel.

The above calculation takes as initial conditions the temperature (T) and relative humidity (RH) that determines the water vapor concentration of the starting air mass. Air starting at the ground with a specific T and RH is lifted along the dry adiabat following (Eqn. 3b) and (Eqn. 4b) with the vapor fraction equal 1.0 until condensation starts at the cloud condensation level when $q = q_s$ (Fig. 4). Condensation then occurs at all levels above the cloud condensation level as described by (Eqn. 3a) and (Eqn. 4a) resulting in progressive decrease in the remaining vapor fraction as a function of adiabatic ascent. Latent heat release associated with condensation changes the temperature lapse rate to a moist adiabat. It is this temperature and the associated phase(s) that controls the equilibrium fractionation between the remaining vapor and condensate as represented by the corresponding α's (Fig. 4). This thermodynamically

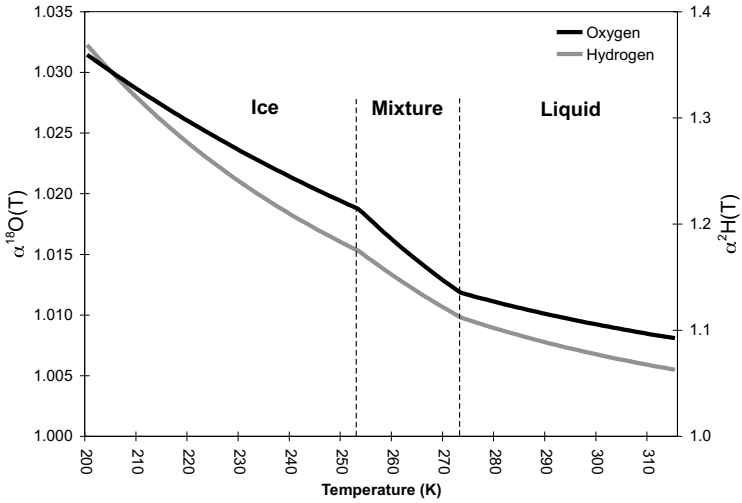

Figure 2. Fractionation factors as a function of temperature as used in the model based on empirical fits determined by (Majoube 1971b; Horita and Wesolowski 1994) and (Merlivat and Nief 1967; Majoube 1971a) See Rowley et al. (2001), Rowley and Garzione (2007) for original publications for the equations graphed in Figure 2.

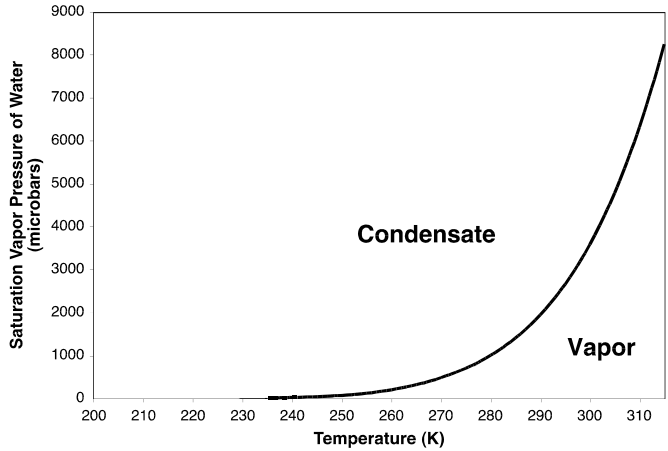

Figure 3. Saturation vapor pressure curved based on a fit to the Smithsonian Tables as a function of temperature.

determined adiabatic lapse rate depends solely on the starting *T* and RH. Therefore, different starting air mass conditions will yield different rates of condensation with elevation and hence $\delta^{18}O$ (δD) vs. altitude relationships. The decreasing water vapor fraction, and hence decreasing ratio of initial to remaining water vapor, with height results in a decrease in the latent heat contribution that together drives the Rayleigh distillation process resulting in the progressive isotopic depletion of the remaining reservoir from which subsequent condensation occurs.

The global mean isotopic lapse rate of precipitation in low latitudes depends sensitively on the initial sea level *T* and RH frequency distribution (Rowley et al. 2001). Coupled monthly mean *T* and RH data derived from NCEP reanalysis output (Kalnay et al. 1996) of 40 years

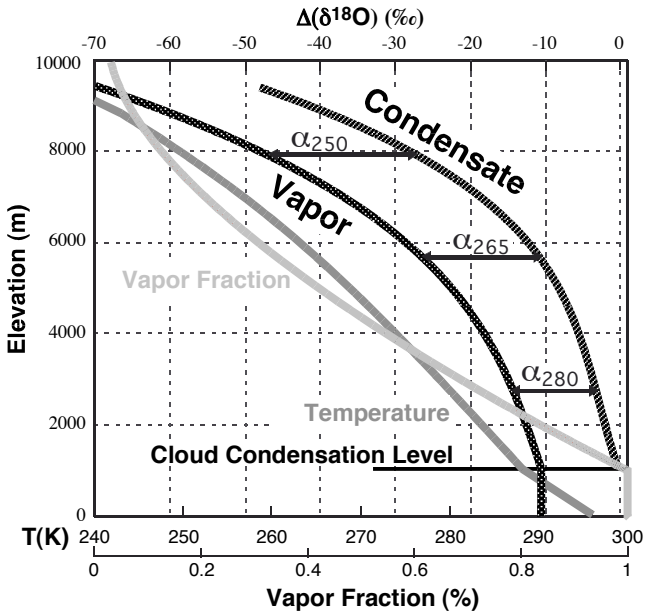

Figure 4. Graph of temperature, vapor fraction, and isotopic composition of water vapor and condensate as a function of elevation for an air mass with a starting *T* and RH of 295 K and 80 % (modified after Rowley and Garzione 2007). Note that the vapor and condensate are the isotopic composition reflected in the scale along the top of the graph with $\Delta(\delta^{18}O)$ normalized relative to the initial isotopic composition of the condensate. The isotopic composition of modeled condensate is not the same as precipitation as is discussed below.

data were extracted from the monthly mean *T* and RH data from all low latitude (≤ 35°N and S), entirely oceanic, 2° × 2° grid cells in the reanalysis product. A total of 614 unique pairs of *T* and RH values, corresponding to 33,168 instances that are taken to represent the likelihood of starting air mass conditions for the model. These define the probability density function of these parameters (see Fig. 2 of Rowley et al. 2001) used to model global mean isotopic lapse rate of precipitation. Rowley et al. (2001) and Rowley and Garzione (2007) used Monte Carlo simulation of 1,000 to 5,000 random pairs to estimate the probability density functions of modeled vertical profiles of temperature and vapor fraction and $\Delta(\delta^{18}Op)$ with respect to elevation. That analysis is updated by using all 33,168 instances to estimate the probability density functions of modeled vertical profiles of temperature and vapor fraction (Fig. 5).

Rowley et al. (2001) derived an empirically-based scheme to convert the isotopic composition of condensate that the model calculates to the isotopic composition of precipitation, which is what is observed. The scheme devised by Rowley et al. (2001) was based on GNIP weighted mean annual isotopic composition of precipitation as a function of elevation in the Alps. The scheme weights the isotopic composition of the condensate as a function of elevation by the condensation amount as a function of elevation within a 1,000 m thick parcel of air between 1,000 and 2,000 m above the ground surface. The precipitation thus calculated represents the condensation amount weighted mean isotopic composition of the modeled condensate extracted from within this kilometer thick parcel of air. This scheme is re-investigated here using data from tropical regions, collected by either Gonfiantini et al. (2001) or released by IAEA in 2004 for the period up to 2001 (IAEA-Monthly 2004; IAEA-Yearly 2004). The observed isotopic compositions are normalized to $\Delta(\delta^{18}Op)$ by subtracting

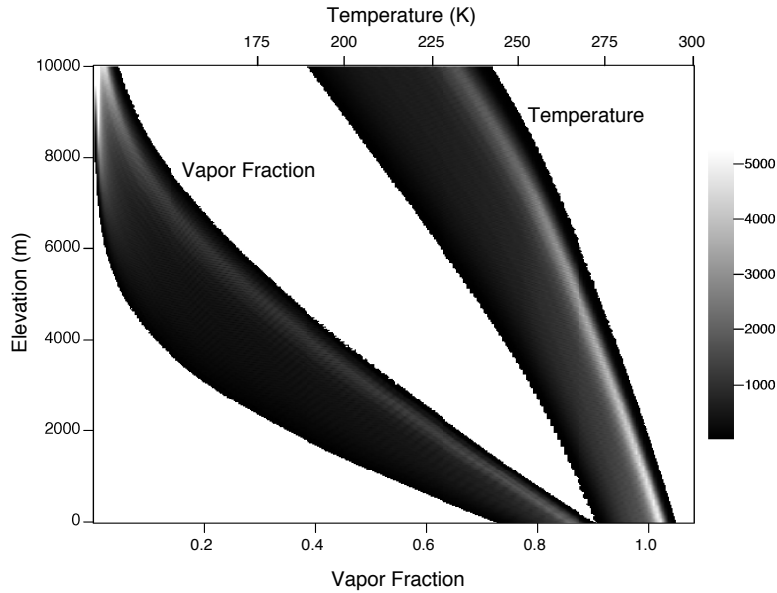

Figure 5. Frequency distribution of modeled condensation weighted mean vapor fraction and temperature relative to elevation. Elevation represents the surface elevation with the frequency representing the modeled parcel 2,000 ± 500 m above the surface from which precipitation falling to the ground is derived. Gray scale color scaled to the number of times a given value of temperature and vapor fraction as a function of elevation is modeled.

an estimate of the low altitude starting weighted mean annual isotopic composition from each of the remaining weighted mean annual isotopic values as listed in Table 1. The starting surface *T* of 299 K and RH of 80% is appropriate for each of the regions so no correction needs to be applied for the analysis. The model is run for this starting *T* and RH and the spectrum of curves for various sampling elevations is computed (Fig. 5, inset). The best fit sampling elevation is determined by minimizing the root mean squared difference between the model-derived predicted isotopic composition and the observed $\Delta(\delta^{18}Op)$ at each of the station elevations listed in Table 1. Based on these data the best-fit sampling elevation for a 1000m thick parcel is located between 1500 m and 2500 m higher than the land surface, that is with a mean elevation of 2000 m higher than the land surface (Fig. 6).

As is clear from the inset figure (Fig. 6) there is little difference at low elevations and so the main controllers of the best-fit solution are the higher altitude stations. This solution is preferable to that used by Rowley et al. (2001) in that the highest sampling station in the Alpine dataset was Grimsel at just over 2000 m, hence not able to tightly constrain the curve, as well as the fact that the sites used here are well within the ±40° latitude band where the model is most appropriately applied.

In the previous analyses Rowley et al. (2001), and derivative papers including Rowley and Currie (2006) and Rowley and Garzione (2007) quoted model results for the weighted mean $\Delta(\delta^{18}O_p)$ as a function of elevation. It turns out that the relationship between $\Delta(\delta^{18}O_p)$ and elevation calculated in Rowley et al. (2001) was the average of $\Delta(\delta^{18}O_p)$ at each elevation, as opposed to the average elevation at each $\Delta(\delta^{18}O_p)$. The confidence intervals, however, were correctly computed in terms of frequency distribution of elevation as a function of $\Delta(\delta^{18}O_p)$. The result of this difference in computation of the median and weighted mean was a significant difference in the predicted elevation based on the weighted mean and the median (see Rowley

Table 1. Weighted mean $\Delta(\delta^{18}O_p)$ versus elevation used to calibrate the sampling elevation of the calculated isotopic composition of condensation versus elevation.

Station	Station Altitude	Weighted Mean $\Delta(\delta^{18}O_p)$	Location	Ref.
Bakingele	10	0.2	Mt. Cameroon	1
Debundscha	20	0.1	Mt. Cameroon	1
Idenau	30	−0.4	Mt. Cameroon	1
Batoki	50	0.1	Mt. Cameroon	1
Brasseries	180	−0.4	Mt. Cameroon	1
Bomana	460	−0.6	Mt. Cameroon	1
Bonakanda	860	−1.4	Mt. Cameroon	1
Foret SW	1000	−1.0	Mt. Cameroon	1
Upper Farm	1100	−1.7	Mt. Cameroon	1
Route VHF	1610	−2.4	Mt. Cameroon	1
Limite Foret SW	2320	−3.9	Mt. Cameroon	1
Station VHF	2460	−3.7	Mt. Cameroon	1
Versant Nord	2475	−3.2	Mt. Cameroon	1
Versant Nord	2500	−3.8	Mt. Cameroon	1
Limite BUEA	2500	−3.4	Mt. Cameroon	1
Hutte 2	2925	−4.4	Mt. Cameroon	1
Versant SW	3000	−4.7	Mt. Cameroon	1
Nord	3050	−4.8	Mt. Cameroon	1
Southwest	3300	−5.4	Mt. Cameroon	1
Sommet Bottle Peak	4050	−6.3	Mt. Cameroon	1
Trinidad	200	0.0	Bolivian Andes	1
Rurrenabaque	300	−0.8	Bolivian Andes	1
Coroico	1700	−3.4	Bolivian Andes	1
Chacaltaya	5200	−10.3	Bolivian Andes	1
El Alto	4080	−9.9	Bolivian Andes	1
Izobamba-Sao Gabriel	3058	−7.2	GNIP Brazil-Peru	2
Bogota-Sao Gabriel	2547	−5.0	GNIP Brazil-Colombia	2

(1) Gonfiantini et al. (2001), (2) (IAEA-Yearly 2004). Mount Cameroon normalized relative to the precipitation amount weighted average isotopic composition of −3.2‰ of the stations below 100 m elevation. Bolivian Andes data normalized to precipitation amount weighted average isotopic composition of −5.2‰ at Trinidad. Izobamba and Bogota are normalized to weighted mean isotopic composition measured at Sao Gabriel of −4.4‰.

et al. 2001-Fig. 8). Figure 7 shows the revised model results in which both the weighted mean and the confidence intervals are computed as averages of elevation at each $\Delta(\delta^{18}O_p)$, and with the revision of the sampling height of the condensate to 2,000±500 m. Included with this figure is the relationship between $\Delta(\delta^{18}O_p)$ and elevation from Rowley et al. (2001) computed with the polynomial fit reported by Currie et al. (2005). These two revisions effectively cancel each other such that the best fit curve with the current scheme is nearly identical with that of Rowley et al. (2001) and Currie et al. (2005). Increasing the mean sampling height effectively systematically lowers the median and $\pm1\sigma$ and $\pm2\sigma$ distributions to correspond with the revised weighted mean curve.

Given that this revised calibration scheme together with the correction of the weighted mean calculation are nearly identical (< ±150 m difference) to the previous model results all of the comparisons of the modern isotopic compositions of precipitation from other regions are effectively unchanged and hence these comparisons demonstrates that the model yields quite reasonable fits without adjustment (see Rowley et al. 2001 and Rowley and Garzione 2007). However it should always be made clear that the empirical scheme to model precipitation from condensate does not represent the microphysics of water droplet formation, coalescence,

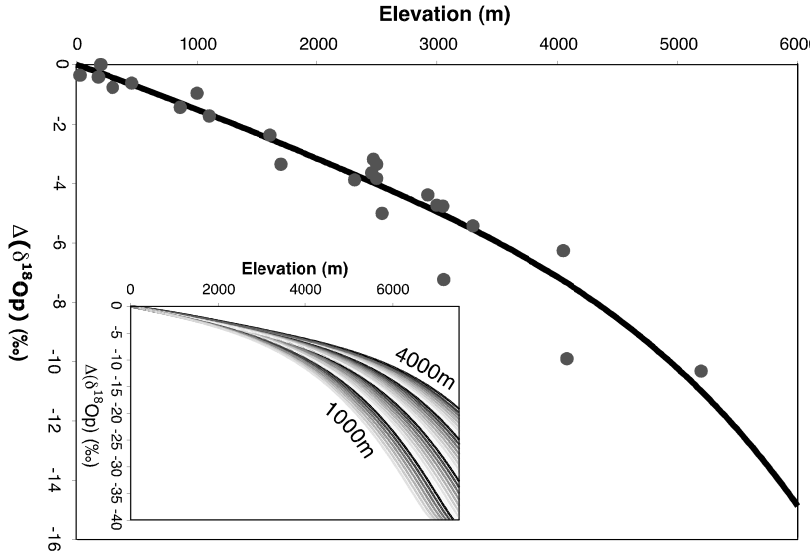

Figure 6. Empirical fit of isotopic composition of condensate sampled from a 1 km thick parcel at a mean elevation 2,000 m above the ground surface. Dots represent data from Table 1. Inset-family of curves representing a range of mean sampling elevations from 1000 to 4000 m above the surface. The best fit curve is at 2000 m elevation above the surface.

turbulent mixing, and eventual fall or re-evaporation within clouds, but rather to simply derive a means of providing an empirical match between condensate and precipitate in orographic settings. Further, many regions, particularly those where significant evaporation occurs during precipitation descent from the level of condensation to the ground will not be fit by this relationship. In the modern world this is readily tested using deviations of precipitation from the global meteoric water line (GMWL) (Craig 1961; Dansgaard 1964) and particular care needs to be taken in applying this or any Rayleigh distillation-based approach in such regions. Evaporation enriches the precipitation in ^{18}O and to a lesser degree ^{2}H making it appear to have condensed at lower elevations. For example, the GNIP station at Addis Abba at 2360 m has an amount weighted mean annual $\Delta(\delta^{18}O_p)$ of about −1.0 ‰, that is more enriched than the mean $\Delta(\delta^{18}O_p)$ of −3.6±1.6‰ for low elevation (≤ 100 m) and low latitude (≤ ±35°) stations in the GNIP database (IAEA-Yearly 2004). Obviously a positive $\Delta(\delta^{18}O_p)$ has no meaning in terms of elevation but can be an indication of evaporative enrichment of ^{18}O.

Polynomial regression of the relationship of $\Delta(\delta^{18}O_p)$ versus elevation (z) measured in meters derived from modeling all possible modern starting T and RH pairs for values of $\Delta(\delta^{18}O_p)$ between 0‰ and −25‰ results in a curve that is only slightly different from the equation reported by Currie et al. (2005) and used by Rowley and Currie (2006), as well as that of Rowley and Garzione (2007). The revision is Equation (5):

$$z_{weighted\ mean} = -0.0129\ \Delta(\delta^{18}O_p)^4 - 1.121\ \Delta(\delta^{18}O_p)^3 - 38.214\ \Delta(\delta^{18}O_p)^2 - 715.22\ \Delta(\delta^{18}O_p) \quad (5)$$

The difference in elevation computed using the equation in Currie et al (2005) and Equation (5) ranges from about +150 to −84 m in the range of the fit. Polynomial regression constrained to pass through the origin of the median of the distribution yields the relationship

$$z_{median} = -0.0168\Delta(\delta^{18}O_p)^4 - 1.368\ \Delta(\delta^{18}O_p)^3 - 43.75\ \Delta(\delta^{18}O_p)^2 - 771.11\Delta(\delta^{18}O_p)$$

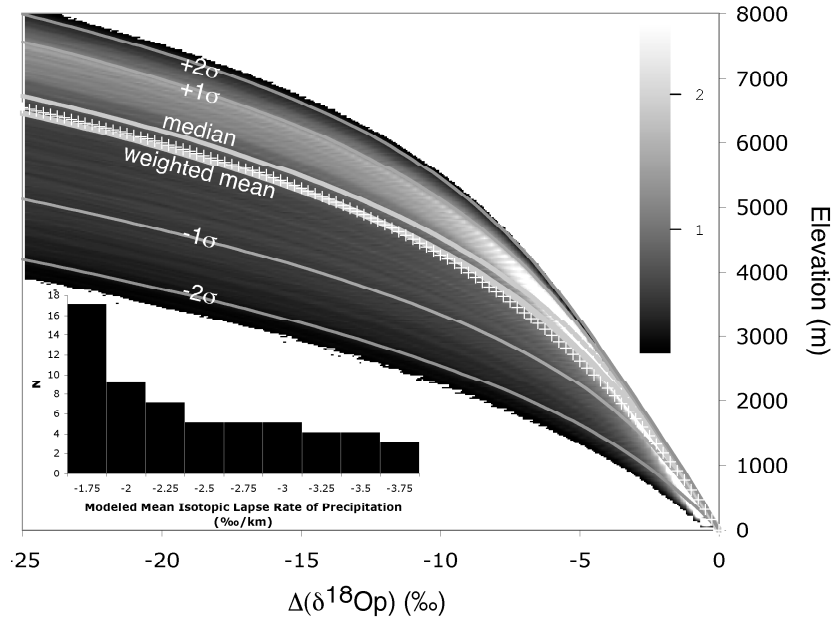

Figure 7. Frequency distribution of $\Delta(\delta^{18}O_p)$ versus elevation derived by weighting all possible pairs of starting *T* and RH and corresponding computed vertical profiles of *T* and vapor fraction shown in Figure 6 by their frequency of occurrence in the Rowley et al (2001) probability density function of *T* and RH. Gray curves highlight the weighted mean (heavy), median, and ±1σ and ±2σ deviations resulting from the probability density distribution of corresponding starting *T* and RH. White pluses are the Rowley et al. (2001) and Currie et al. (2005) values of the $\Delta(\delta^{18}O_p)$ versus weighted mean elevation. Gray scale shading in percent, saturating to white above 3%. Note that warmer starting temperatures plot in the +σ direction whereas colder starting temperatures plot in the −σ direction. Any change in mean global climate, and particularly in low latitude mean and variation of sea level temperature will affect the mean lapse rate of isotopic composition in a similar direction. Inset histogram - modeled isotopic lapse rates of $\Delta(\delta^{18}O_p)$ derived from the model for elevations between 1500 m and 6500 m.

It has long been understood that starting temperature has a much larger effect on the isotopic lapse rate than does relative humidity, hence the wide utilization of isotopic composition of snow and ice to derive estimates of temperature variation (Dansgaard 1964). Given that the lapse rate of isotopic compositions is, according to the model, primarily dependent upon starting temperature and secondarily relative humidity (see Rowley and Garzione 2007), and given that the mean starting temperature and relative humidity of air masses in the past are not known, a reasonable estimate of elevation uncertainty is provided by the frequency distribution of $\Delta(\delta^{18}O_p)$ versus elevation values (Fig. 7). Accordingly estimates of the elevation uncertainty relative to the weighted mean elevation are shown in Figure 8 and given by the following fits to the model frequency distribution:

$$z_{+2\sigma\ uncertainty} = 0.0228\Delta(\delta^{18}O_p)^4 + 1.132\Delta(\delta^{18}O_p)^3 + 14.276\Delta(\delta^{18}O_p)^2 - 57.547\Delta(\delta^{18}O_p)$$

$$z_{+1\sigma\ uncertainty} = 0.0150\Delta(\delta^{18}O_p)^4 + 0.738\Delta(\delta^{18}O_p)^3 + 9.031\Delta(\delta^{18}O_p)^2 - 47.186\Delta(\delta^{18}O_p)$$

$$z_{-1\sigma\ uncertainty} = -0.0126\Delta(\delta^{18}O_p)^4 - 0.580\Delta(\delta^{18}O_p)^3 - 5.262\Delta(\delta^{18}O_p)^2 + 89.212\Delta(\delta^{18}O_p)$$

$$z_{-2\sigma\ uncertainty} = -0.0023\Delta(\delta^{18}O_p)^4 + 0.107\Delta(\delta^{18}O_p)^3 + 11.611\Delta(\delta^{18}O_p)^2 + 280.09\Delta(\delta^{18}O_p)$$

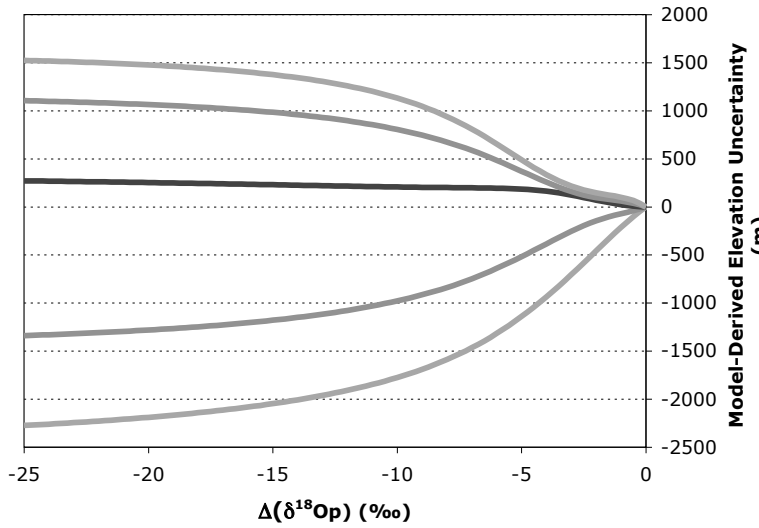

Figure 8. Model-derived elevation uncertainty relative to the weighted mean elevation as a function of $\Delta(\delta^{18}O_p)$ resulting from uncertainty in the starting *T* and RH of orographically forced ascent of airmasses. Curves are ±1σ (light gray), ±2σ (medium gray). The difference between the median (dark gray) and weighted mean is also shown.

Why are these equations represented by 4th order polynomials and not 2nd order curves given that the vertical variation of temperature and vapor fraction are well approximated by second order functions? The simple answer is that the transition from condensing water vapor to liquid water above 0 °C to condensing water ice below −20 °C, and the attendant affect on the fractionation factor (Fig. 2), results in additional structure not captured by 2nd or 3rd order curves. Each of the equations fit their respective model output with an $R^2 > 0.9997$. The lack of symmetry of the modeled uncertainty reflects asymmetry in the probability density function and particularly the long tail toward lower values of T relative to the mean (see Fig. 2 of Rowley et al. 2001). The effect of this long tail is well displayed in both Figure 5 and 7.

The thermodynamic model that determines the theoretical $\delta^{18}O$ (δ^2H) vs. altitude relationship is mathematically one-dimensional, in that the equations need only be integrated with respect to ζ. The vertical trajectories themselves can wander horizontally in an arbitrarily complex way as the parcel ascends. The chief physical assumption is that the air parcel remains relatively isolated from the surrounding air. Although turbulence, among other processes, no doubt contribute to isotopic lapse rates of precipitation in real world orographic settings, the fit of observed isotopic lapse rates with model predictions implies that the model captures the main features determining the relationship between elevation and isotopic composition in many low latitude settings (Rowley et al. 2001; Rowley and Garzione 2007).

Climate change, and particularly changes in mean sea level temperatures have the potential to significantly affect isotopic lapse rates in the past. Figure 9 compares results using the modern low latitude distribution of climate parameters with those derived from GCM model output of Eocene (Huber and Caballero 2003) conditions to demonstrate this point. On average most estimates of past climate suggest that the Present is more toward the colder end of the climate spectrum and thus most times in the past, such as the Eocene would have been warmer with potentially slightly higher sea surface relative humidity, resulting in lower isotopic lapse rates in the past. This illustrates an important aspect of having a model rather than simply employing an empirical calibration of the isotopic lapse rate (see for example Chamberlain

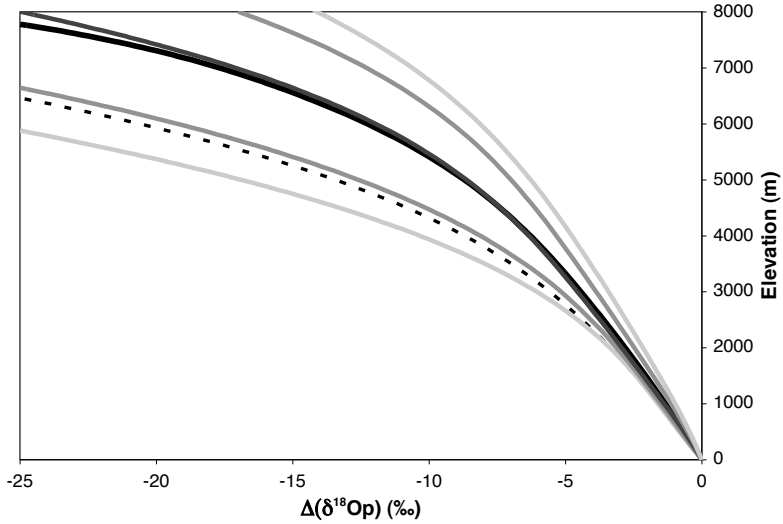

Figure 9. Comparison of modeled Eocene (heavy black curve) and modern (dashed black curve) weighted mean $\Delta(\delta^{18}O_p)$ versus elevation relationships. The warmer (T_{mean}=300 K ± 3 K (1σ), RH $_{mean}$= 80% ± 3% (1σ)) climate of the Eocene modeled by Huber and Caballero (2003) results in a lower isotopic lapse rate predicted for this time. The median (dark gray), and ±1σ (medium gray), and ±2σ curves (light gray) appropriate for the Eocene low latitude climate are also shown. For comparison the modern +2σ curve (Fig. 7) and the Eocene median curve are essentially identical. Comparable predicted isotopic lapse rates can be calculated for any given time for which GCM-derived climate parameters are available. Note the isotopic lapse rate is ‰/m and thus is the inverse of this graph.

and Poage 2000; Garzione et al. 2000a,b, 2006; Poage and Chamberlain 2001). There is no quantitative way to derive the magnitude of the effect of climate change on empirical isotopic lapse rates. One of the nice aspects of having a model is that it is possible to recalculate the relationship between $\Delta(\delta^{18}O_p)$ and elevation, if appropriate GCM derived model results are available. Since the required data are sea level *T* and RH over oceanic regions rather than continental interiors these data are probably less affected by details of elevation reconstructions within continental interiors and hence less likely to circularly affect the model results for 1D predictions of the isotopic lapse rate.

Figure 9 very nicely demonstrates the effects of global climate change on the isotopic lapse rate. Warmer climates yield shallower isotopic lapse rates while colder, drier climates would be expected to be associated with steeper isotopic lapse rates. On average much of the geologic past is generally assumed to have been warmer and hence application of the mean modern lapse rate will underestimate paleoelevations in these cases.

MODEL VERSUS EMPIRICAL FITTING OF DATA

The model suggests that there should be considerable sensitivity of the isotopic lapse rate to temperature of low elevation air mass from which precipitation is derived. Rowley and Garzione (2007) illustrated this by comparing profiles of $\Delta(\delta^{18}O_p)$ versus elevation for Mount Cameroon based on the data reported by Gonfiantini et al. (2001). The 4 K change in *T* between the mean of the probability density function of *T* and RH at 295 K and locally appropriate value of 299 K results in a significant improvement in the correlation between data and model predictions (See Fig. 5 of Rowley and Garzione 2007). Empirical calibration of

the isotopic lapse rate using temporally limited sampling will almost invariably underestimate the potential range of variability in isotopic composition as a function of elevation, reflecting the limited range of climate variability represented by those samples. Temporally limited sampling can refer to a single suite of samples collected within a month or so from relatively short streams (e.g., Garzione et al. 2000a,b), or precipitation data collected over less than 28 months (Gonfiantini et al. 2001) of which only one year of the data were used by Garzione et al. (2006), to compilations of river data collected over a range of time scales by different sources as in Poage and Chamberlain (2001). Even the GNIP data (IAEA-yearly 2004) with up to several decades of measurements are potentially temporally limited relative to climatological means. Thus, although a good fit between isotopic composition and elevation may be apparent in each of these data sets, it is not clear how well any of these data sets captures realistic estimates of their respective climatological means. This comment extends to estimates of elevation uncertainty that are typically based on bootstrapping of deviations of observations about the best-fit regression relationship (see Rowley and Garzione 2007). The model, in contrast, represents an ensemble mean that captures the sort of variability expected in low latitude situations. The climatic conditions represented in the model can easily be either perturbed by specifying a constant offset in ΔT and or ΔRH, or use a new probability distribution function of T and RH, based, for example, on GCM output to recalibrate the $\Delta(\delta^{18}O_p)$-elevation relationship (Fig. 9). This cannot be done rigorously with empirical calibrations.

To make this point clearer, the data from Gonfiantini et al. (2001) provides an instructive data set for thinking about issues related to limited temporal sampling and empirical fitting. Gonfiantini et al. (2001) report station elevation and $\delta^{18}O_p$ on a monthly basis for some number of months between December 1982 to April 1986. They also report temperature and precipitation amount for some subset of these months and stations, along a transect from the Bolvian foreland to the Altiplano, from Trinadad to El Alto (see their Table 6). This data set essentially provides six different, although not independent, measures of the relationship between elevation and isotopic composition (Fig. 10). These are unweighted and precipitation amount weighted mean $\delta^{18}O_p$ that are combined into a 1983, 1984, and December 1982 through part of April 1986 average data sets. The 1984 unweighted means, listed incorrectly in Gonfiantini et al. (2001) Table 5 as weighted means, were regressed by Garzione et al. (2006) as corrected in Garzione et al. (2007) in order to constrain their estimate of the paleoelevation history of this part of the Bolivian Altiplano as shown by the dashed curve in Figure 10. Several things are immediately apparent. There are significant differences depending on how the data are combined. The 1984 isotopic compositions, representing up to 11 months of data are significantly more depleted than either 1983, based on between 9 and 12 months of data, or the combined 1982 to 1986 average isotopic compositions, based on between 15 and 27 months of data. Amount weighted means are, on average, more depleted than unweighted means by as much as several per mil. On the basis of these data there is no basis for judging whether any of these data represent the climatological mean relationship. Garzione et al. (2007) prefer regressing the weighted mean of all existing data (bold line in Fig. 10) because it more closely matches isotopic compositions of tributaries collected in 2004 and 2005, but additional data may suggest some other relationship within or beyond the existing data is more representative. Thus my preference for comparing observation against the model, and to use the uncertainties in elevation represented by climate variation embedded in the model to estimate paleoaltitude uncertainties in the past.

One final point regarding Figure 10 is that each of the data sets internally yield comparable isotopic lapse rates, i.e., they are characterized by similar slopes, but significantly different 0 m $\delta^{18}O_p$ intercept values. This emphasizes the important point that it is not the absolute value of the $\delta^{18}O_p$ that correlates with elevation, but rather the difference relative to low elevation starting isotopic composition, and hence the importance of normalizing in terms of $\Delta(\delta^{18}O_p)$, rather than modeling in terms of measured $\delta^{18}O_p$.

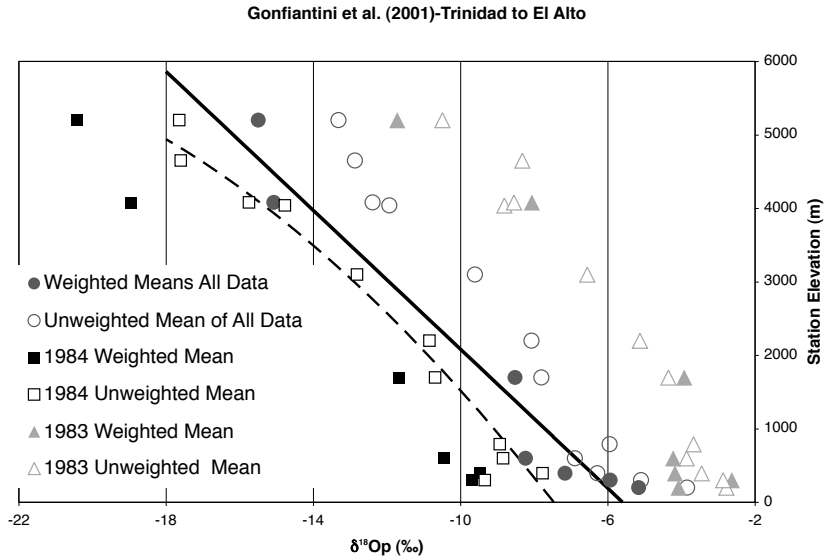

Figure 10. $\delta^{18}O_p$ versus elevation for various groupings of the data presented by Gondiantini et al. (2001) based on data in their Table 6. Black dashed curve is the polynomial regression curve derived from the unweighted mean isotopic composition as a function of elevation used by Garzione et al. (2006) as corrected by Garzione et al. (2007) and the bold line is the linear regression relationship preferred by Garzione et al. (2007).

How does the model compare with various previous empirically derived estimates of the relationship between isotopic composition and elevation, either globally (Poage and Chamberlain 2001), or locally in the Himalayas (Garzione et al. 2000a,b), or in the eastern Andes (Garzione et al. 2006, 2007) (Fig. 11). Garzione et al. (2000b) already compared their fit with an early version of the model, later published as Rowley et al. (2001), and noted the similarity. It is clear from the comparison presented in Figure 11 that there is first-order agreement among these different approaches. The necessary underlying assumption for the empirical fits is that the existing samples represent the long-term climatological means, but as demonstrated above there is no basis for judging how true this is and hence bootstrapping of deviations from best fit relations also likely significantly underestimates uncertainties. The model provides an independent basis for estimating the likely mean and variations in this relationship, and hence provides a more robust estimate of inherent uncertainty than estimated by bootstrapping of a given data set alone.

DATA-MODEL COMPARISONS

Rowley et al. (2001), Currie et al. (2005), Rowley and Currie (2006), and Rowley and Garzione (2007) have reviewed various comparisons of modern day observed isotopic compositions with those predicted by application of this model. For the most part these comparisons have been quite favorable with a fairly close (± ~500 m) match between known and predicted elevations. In the next section additional comparisons are made between various model predictions relative to observed data from the modern world where there is essentially no uncertainty in either the measured isotopic composition or the elevations of various samples.

The discussion below specifically focuses on application of the model to low latitude (<35°N or S) examples, in order to further validate the global model. There are several reasons for emphasizing this latitude range and not higher latitudes. First, tropical latitudes are more

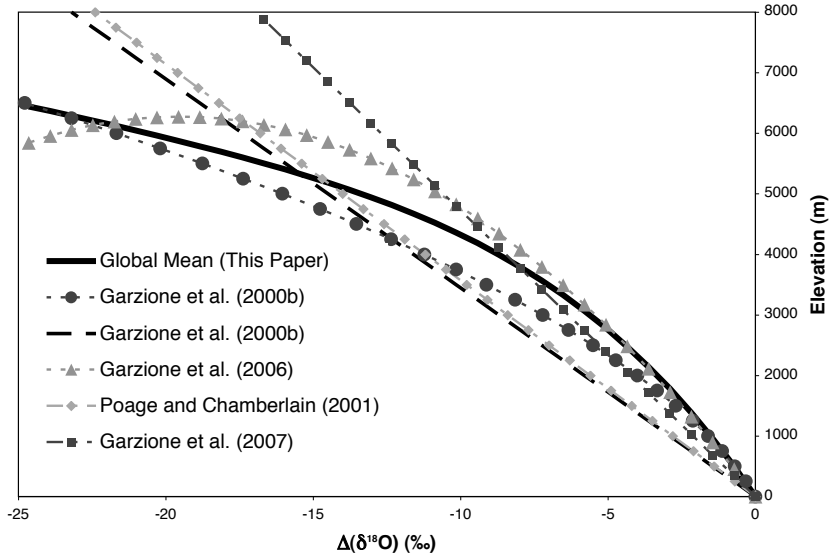

Figure 11. Comparison among a variety of empirically derived estimates of the relationship between $\Delta(\delta^{18}O)$ and elevation. Note that Poage and Chamberlain (2001) and Garzone et al. (2000b) are fits to rivers, not precipitation, hence it is not surprising that in the range of $\Delta(\delta^{18}O)$ values that constrain their estimates that the slopes are less than that predicted for precipitation. The mean climate in the Bolivian Andes transect is about 4 °C warmer than the global mean of the T and RH probability density function, giving rise to the steeper slope of the Garzione et al. (2006) and Garzione et al. (2007) curve than the global mean curve, as shown by Rowley and Garzione (2007).

likely to derive moisture from within these latitudes and hence are well represented by the *T* and RH probability density distribution used in the model to estimate isotopic lapse rates. Second, strong latitudinal temperature gradients in oceanic source areas at latitudes poleward of about 40° result in significant increase in *T* variability and hence in variability of estimated isotopic lapse rates at higher latitudes (Rowley and Garzione 2007). Third, mid-latitude and temperate systems are typically characterized by complex frontal systems and air mass mixing with potentially multiple independent moisture sources each with different isotopic, *T* and RH characteristics, resulting in much more complex initial starting conditions than is captured in our simple one-dimensional model. We thus restrict our discussion to regions within ±35° of the equator. Even within this latitude range, complex vapor trajectories exist giving rise to complex patterns in the isotopic compositions (Friedman et al. 2002a,b).

It is critical to assess the fit of the model to modern systems for which the first-order isotopic composition as a function of elevation has been determined empirically, before any confidence is warranted in the application of this model or for that matter other empirical approaches predicated on application of the same thermodynamic rationale (Garzione et al. 2000a,b) for paleoaltimetry studies. The most robust statistic of the isotopic composition at any given station is the precipitation amount weighted annual mean. This reflects the fact that there is considerable variability in isotopic composition as a function of hour, day, month or season at most stations and hence the comparison that needs to be made is preferably with a multi-decadal record or at least with multi-year records wherever possible. Similarly, surface waters generally integrate the isotopic composition over the mean residence time within the drainage basin and would also be expected to reflect the amounts of precipitation as a function of time rather than just its average isotopic composition. In the following discussion attention will be focused entirely on amount weighted isotopic compositions, unless data on this quantity are

not available. Rowley and Garzione (2007) presented comparisons for precipitation collected from altitude transects up Mount Cameroon and Bolivian Andes from Gonfiantini et al. (2001), and Himalaya-Southern Tibet. In this discussion additional data from the Himalayan region will be reviewed. The primary focus will be Himalayan rivers.

However, in order to bring some closure in regards the above discussion regarding the Bolivian Andes data (Gonfiantini et al. 2001) a comparison is presented of these various data sets in relation to the model (Fig. 12). Each of the data sets, the weighted mean isotopic compositions for 1983, 1984, and the average for the interval from 1982 to 1986 as derived from Table 6, rather than Table 5, of Gonfiantini et al. (2001) are normalized relative to the 0 m intercept of linear regressions of each subset of station elevation against $\delta^{18}O_p$, so that they are plotted as $\Delta(\delta^{18}O_p)$. Also included are the isotopic compositions of small tributaries with samples from 2004 and 2005 as a function of elevation from Garzione et al. (2007). The small tributaries are normalized relative to the 0 m intercept of a linear regression of sample elevation against $\delta^{18}O_{mw}$. Figure 12 demonstrates that the model captures the first-order relationships reflected in these various data sets, tends to underestimate the elevations of the highest stream samples, as expected given the 4 °C difference between the global climatological mean and the best estimate of the local climatological mean. In addition, it would appear that 1983 was indeed an anomalous year as suggested by Gonfiantini et al. (2001).

SURFACE WATERS

All archives that might be used for paleoaltimetric purposes derive their isotopic signatures either from surface or ground waters rather than precipitation directly. The isotopic composition of surface waters in particular, and ground waters to a lesser degree can differ significantly from

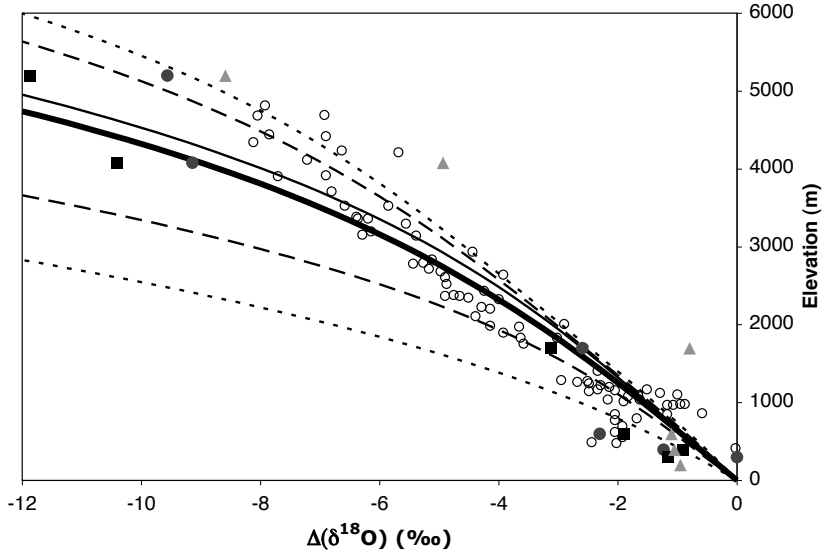

Figure 12. Comparison of normalized isotopic composition of weighted means versus elevation of Bolivian stations from Gonfiantini et al. (2001) for 1983 (triangles), 1984 (squares), and 1982 to 1986 averages (filled circles), and normalized δ^{18}Osw from small tributaries from Garzione et al. (2007) plotted at sample elevations. Model curves are weighted mean (bold), median (fine), ± 1σ (coarse dashed), and ±2σ (fine dashed). Note that detailed location data needed to compute various hypsometric weighted means as discussed below are not yet published for these surface waters.

that of precipitation. The most important difference between surface or ground waters and precipitation is that rivers and streams integrate precipitation in the drainage basins above the point that a sample is taken (Ramesh and Sarin 1995). Surface waters thus integrate (1) variation of isotopic composition with elevation, (2) area as a function of elevation (i.e., hypsometry), as well as (3) variation in precipitation amount as a function of elevation, in addition to seasonal variations. Hypsometry in drainage systems is not a simple linear function of elevation and hence cannot be represented by the average of the maximum and sample elevation (Fig. 10). Rather the hypsometry of each drainage system needs to be computed individually. One consequence of this hypsometric effect is that isotopic compositions along rivers and streams should not be expected to vary in a simple linear fashion with elevation. This is nicely demonstrated by the individual profiles in the compilation of (Poage and Chamberlain 2001), even though those authors limited their treatment of these data to determining the best fit linear slope.

Precipitation amount also varies as a function of elevation, sometimes with strong gradients in orographic systems, particularly at relatively low elevations (< 3-4 km) (Burbank et al. 2003; Putkonen 2004). Anders et al. (2006) and Roe (2005) have provided a large-scale mapping of precipitation rate as a function of orography in the Himalaya and southernmost Tibet using Tropical Rainfall Measurement Mission (TRMM) satellite data. They model the precipitation as a function of elevation as a combination of the change in saturation vapor pressure as a function of temperature (and hence elevation) and surface slope (Roe et al. 2002; Anders et al. 2006). Rowley and Garzione (2007) show that both the weighted mean annual precipitation and median annual precipitation amount decreases linearly with increasing elevation above about 1,000 m. Regression of the TRMM data from Anders et al. (2006) results in Equation (6) describing the relationship between mean annual precipitation amount (P_z in mm/yr) and elevation (z) in meters up to 4,600 m:

$$P_z = -0.172 \pm 0.006z + 869.7 \pm 22.6 \text{ with an } R^2 = 0.9684 \quad (6)$$

as shown by Rowley and Garzione (2007). Above about 4600 m, MAP is approximately constant at about 74 mm/yr. Anders et al. (2006) demonstrate that this relationship accords with a dominant correlation to the rate of condensation as a function of temperature largely controlled by the shape of the water saturation vapor pressure curve (Roe et al. 2002; Anders et al. 2006).

Data from an array of drainages within the Himalayas and associated Indo-Gangetic plain are analyzed in order to gain some appreciation of the relationships among oxygen isotopic composition, basin hypsometry, and precipitation amount all of which vary as a function of elevation. Locations and sampling elevations of isotopic compositions of rivers and streams within this region have been reported by a number of studies (Ramesh and Sarin, 1995; Gajurel et al. 2006, among others) that provide a basis for examination of these relationships (Fig. 13). For each sampling location, GIS-based hydrologic tools are used to compute the drainage basin area, maximum elevation, and hypsometry (i.e., area as a function of elevation) above the reported sample elevation based on Asian Hydro1K digital elevation data (Hydro1k 2005), a USGS product, produced by the EROS Data Center. The hypsometric mean elevation (z_{hm}) of the drainage basin is simply the area weighted mean elevation as a function (z) of elevation as given by Equation (7),

$$z_{hm} = \frac{\sum A_z z}{\sum A_z} \quad (7)$$

with the summations extending from the sample elevation (z_{min}) to the maximum elevation (z_{max}) in the drainage basin. The precipitation weighted mean elevation (Eqn. 8) is computed by weighting the area as a function of elevation (A_z) within the drainage basin by the precipitation

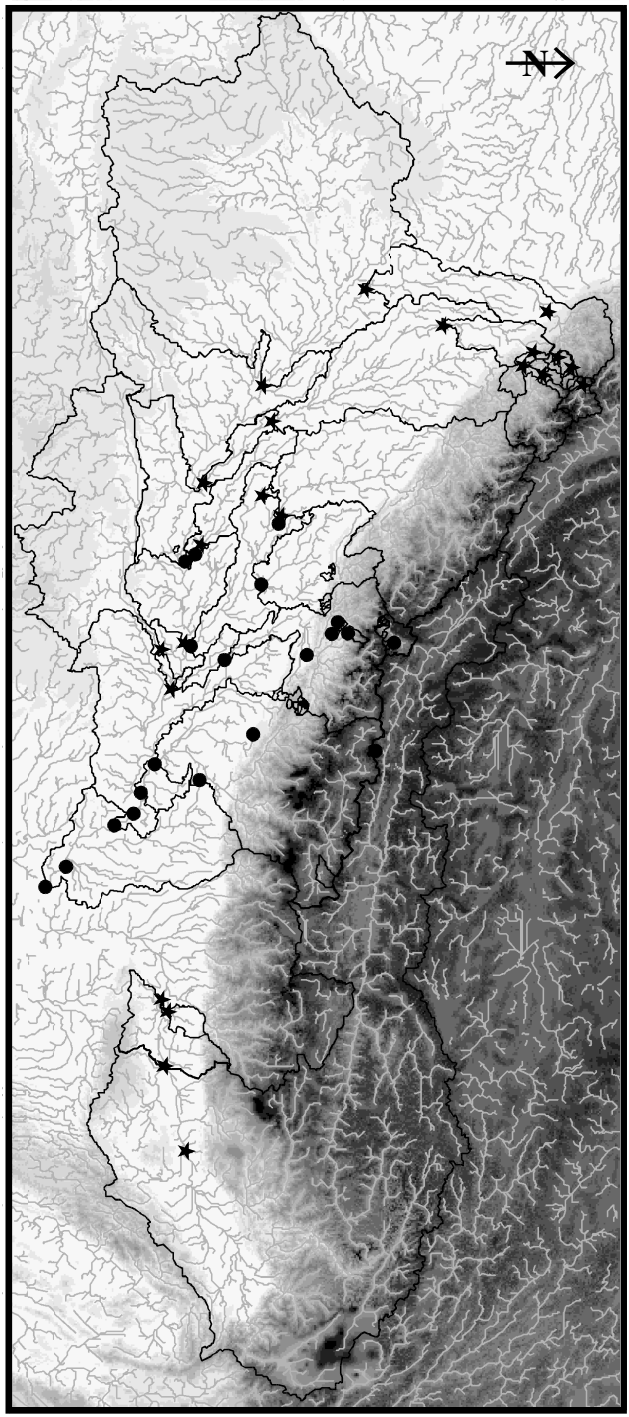

Figure 13. Selection of oxygen isotopic sample localities from the Himalayas and Indo-Gangetic Plain together with outlines of selected associated drainage basins. Stars are primarily from Ranesh and Sarin (1995), filled circles from Gajurel et al. (2006). Rivers and streams and underlying topography derived from Hydro1k digital elevation dataset (Hydro1k 2005). North is to the right.

amount as a function of elevation (P_z), again with the summations extending from z_{min} to z_{max} in the drainage basin.

$$z_{pwm} = \frac{\sum P_z A_z z}{\sum P_z A_z} \tag{8}$$

Figure 14 plots these for a selection of rivers draining the Himalaya and Indo-Gangetic Plain. The important point to emphasize is that the hypsometric mean elevation of each of the drainages plots to the left of the line of 1:1 correlation. The drainage basin area weighted mean difference between z_{pwm} and z_{hm} exceeds 800 m. Further, for low elevation sampling locations there is typically a marked difference between both the hypsometric mean and precipitation weighted mean elevations and the average (i.e., (maximum + sample)/2) elevation of the drainage basin. This difference decreases as basin area decreases and sampling elevation within the larger drainages increases.

The isotopic composition of surface water, $\Delta(\delta^{18}O_{sw})$, at any given height within a drainage basin should reflect the hypsometry of the drainage basin above the sampling site (A_z) integrated with the amount of precipitation falling as a function of elevation (P_z) on that hypsometry and the progressive decrease in isotopic composition of the precipitation $\Delta(\delta^{18}O_p)_z$ with elevation as given by Equation (9),

$$\Delta(\delta^{18}O_{sw}) = \frac{\sum P_z A_z \Delta(\delta^{18}O_p)_z}{\sum P_z A_z} \tag{9}$$

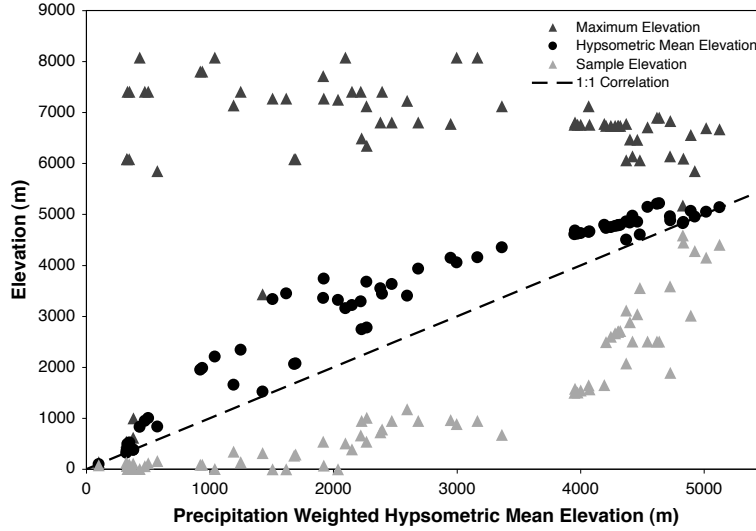

Figure 14. Comparison of hypsometric mean and precipitation amount weighted hypsometric mean elevation for a selection of drainage basins with areas greater than 1,000 km^2 and up to 610,891 km^2 in the Himalaya and southern Tibetan region. Also shown are the sample elevation and maximum elevation within that drainage basin. The sample, hypsometric mean, and maximum elevation of each of the drainages is plotted at the computed precipitation amount weighted hypsometric mean elevation of that drainage basin. The straight dashed line shows the line of 1:1 correlation of the hypsometric mean and precipitation weighted hypsometric mean elevation. The horizontal offset of dots from this line measures the mismatch between these two measures of basin hyspsometry. The mismatch between the precipitation weighted hypsometric mean and the average of the maximum and sample elevation would be even larger (not plotted), particularly for the large rivers sampled in Indo-Gangetic plain that plot on the left side of the graph.

where

$$\Delta(\delta^{18}O_p)_z = -7.293\times10^{-15}z^4 - 6.906\times10^{-12}z^3 - 5.517\times10^{-9}z^2 - 1.577\times10^{-3}z$$

is the polynomial fit of the weighted mean $\Delta(\delta^{18}O_p)_z$ with elevation. An alternative way of looking at this is that the isotopic composition of a river or stream sample should record the z_{pwm} of the drainage basin. For our purposes we compare surface data with various measures of the hypsometry. For the Himalayas, surface water isotopic compositions are compared with precipitation amount modeled with Equation (6). In other areas where a mapping of precipitation amount as a function of elevation is lacking this can be replaced with the condensation weighted hypsometric mean elevation z_{cwm} given by

$$z_{cwm} = \frac{\sum C_z A_z z}{\sum C_z A_z} \tag{10}$$

where the condensation rate C_z as a function of elevation based on the model can reasonably be approximated with:

$$C_z = 1.699\times10^{-8}z + 1.599 \tag{10a}$$

Comparison of z_{pwm} and z_{cwm} is shown in Figure 15. Reiterating that one consequence of this hypsometric effect is that isotopic compositions along rivers and streams should not be expected to vary in a simple linear fashion nor, as pointed out by (Ramesh and Sarin 1995), should the isotopic lapse rate of precipitation and the isotopic lapse rate determined from surface waters be the same. Thus the early analysis of Chamberlain and Poage (2000) trying to constrain the "global" isotopic lapse rate by combining data from precipitation, surface water, and groundwater samples is not appropriate.

Quite extensive data sets exist for the Himalaya–Southern Tibet region. Below we summarize findings derived from analysis of some of these data in the context of the model presented above. The approach taken here is different from that adopted by (Garzione et al. 2000a,b) who derived the isotopic lapse rate by empirically fitting a curve to observed surface

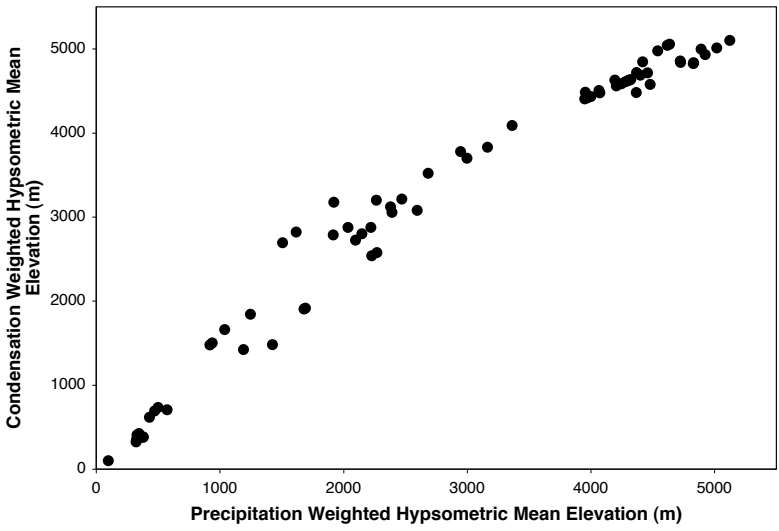

Figure 15. Comparison of the precipitation (z_{pwm}) and condensation (z_{cwm}) weighted hypsometric mean elevations of a selection of Himalayan and southern Tibet drainage basins.

water data. Here the model is used to predict z_{pwm} from the measured $\delta^{18}O_{sw}$ of each sample normalized relative to the amount weighted mean isotopic composition of New Delhi (−5.59‰) to yield $\Delta(\delta^{18}O)$. Predicted z_{pwm} is compared directly with z_{hm} derived from digital elevation data of these drainages (Fig. 16). The close correlation shown by Figure 16 demonstrates that the isotopic compositions of these small drainages are behaving as predicted and that apparent differences between the Seti (Garzione et al. 2000a) and Kali Gandaki (Garzione et al. 2000b) derived lapse rates potentially reflects differences in the precipitation weighted hypsometries of these different drainages as shown by the equally close fit of these two data sets.

One further factor that needs to be taken into account when examining modern surface water data is the seasonal variability in precipitation amount and its isotopic composition. For example, in the case of New Delhi, where, as with much of the Himalayas and southern Tibet, the precipitation regime is dominated by the summer monsoon, there is almost a factor of 40 difference in precipitation amount of the rainiest and driest months of the year, while the isotopic composition varies from around −1‰ during non-monsoon months to as low as −9.3‰ during the monsoon, based on monthly means calculated from 34 years of data for the 1961 to 2001 interval of precipitation records from New Delhi (IAEA-Monthly 2004) (Fig. 17). New Delhi's amount weighted mean annual isotopic composition during this interval is −5.59 ± 0.76‰ (2σ) based on weighting the annual means (IAEA-Yearly 2004). Comparable monthly variability is evident in one year of data from Katmandu (Gajurel et al. 2006). The monsoon season weighted mean isotopic composition at New Delhi is −5.89‰ based on the monthly summary (IAEA-Monthly 2004), hence not different from the annual weighted mean isotopic composition. The effect of significant seasonal variability is potentially most significant in small, short-residence time, drainage basins relative to larger drainages with longer mean residence times.

Rivers and streams not only integrate the precipitation amount weighted hypsometric mean elevation of the drainage basin above the sampling site, but also the seasonal variation in the isotopic composition of the precipitation falling on that watershed. This will be most

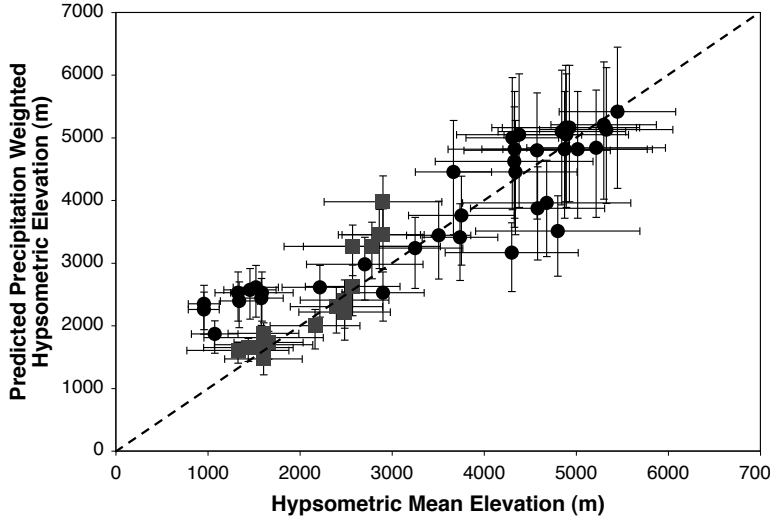

Figure 16. Predicted z_{pwm} vs. Hydro1K-derived (Hydro1k 2005) z_{hm} for the small Himalayan tributary streams of the Seti (Gray squares) and Kali Gandaki (black filled circles) from Garzione et al. (2000a,b). Predicted z_{pwm} is estimated from the measured isotopic composition with ±1σ model uncertainties, and ±1σ deviations about the hypsometric mean elevation. Note from Figure 14 that as the drainage basin decreases in size and as the sample elevation increases that z_{pwm} and z_{hm} become essentially identical.

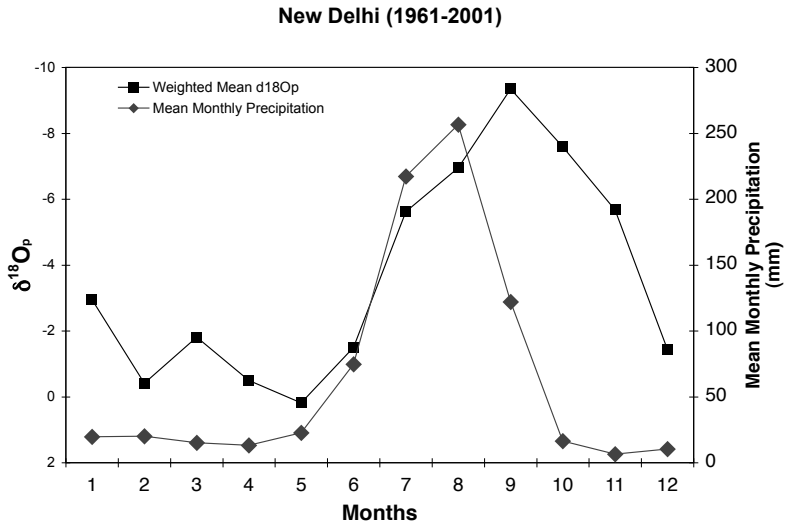

Figure 17. Precipitation amount and amount weighted monthly mean isotopic composition of rainfall in New Delhi from 1961 to 2001 (IAEA-Monthly 2004).

apparent in rivers and streams with short residence times. Given that there are typically only one or at most a few samples from a given sampling location, existing isotopic data from rivers may, but more likely will not reflect the climatological mean isotopic composition of precipitation falling on that watershed. The expected result based on the limited sampling currently available will be a much larger scatter of modern data than would presumably be the case with samples representative of the long-term means.

The discussion below focuses on results summarized from a range of major studies of Himalayan and Ganges rivers by Gajurel et al. (2006). Figure 13 shows sample locations and a subset of the associated drainage basins derived from the Hydro1k hydrologically corrected digital elevation dataset (Hydro1k 2005). In all discussions the measured isotopic compositions are normalized with the 40 year amount weighted mean isotopic composition of precipitation falling in New Delhi to provide an estimate of $\Delta(\delta^{18}O_{mw})$.

Gajurel et al. (2006) summarize isotopic compositions from an array of locations ranging from small drainages well within the Himalayas to samples collected at various locations along the courses of the major rivers within the Ganges plain. These rivers sample a broad spectrum of the hypsometry of this region as reflected in Figure 18, where data on the hypsometric mean elevation, sample elevation, maximum drainage basin elevation are plotted for each sample. Also plotted are the computed z_{pwm} and z_{cwm} for each watershed above the sample elevation. Finally for each sample a model based prediction z_{pwm} based on the reported isotopic composition normalized to New Delhi is plotted.

Rowley and Garzione (2007) presented a comparison of the hypsometry of several large rivers draining the Himalayas with that predicted by measured isotopic compositions reported by Ramesh and Sarin (1995). That comparison was quite favorable, implying that the isotopic composition of foreland basin rivers can indeed record the precipitation weighted hypsometric mean elevation of their drainages. This suggests that it may be possible to discern aspects of orography from foreland basin records in ancient orogenic systems. Rowley and Garzione (2007) noted that due to the strong influence of the precipitation weighting that the isotopic compositions can not be used to say much more than that elevated topography exists, but that

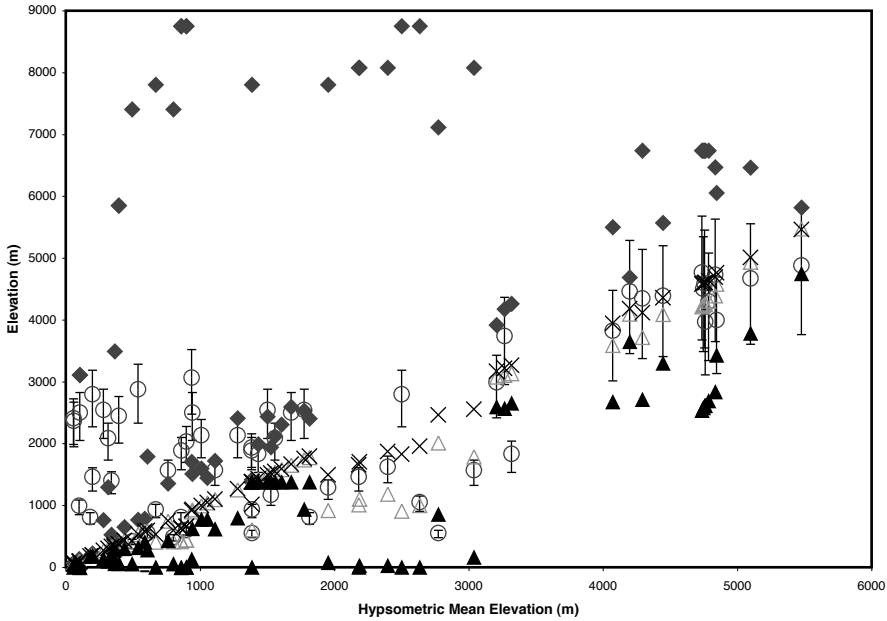

Figure 18. Comparison of various measures of drainage basin hypsometry with the predicted elevation of the precipitation weighted hypsometric mean elevation (black circles) for a selection of river compositions reported by Gajurel et al. (2006). The vertical bars are model-derived ±1σ confidences in the predicted elevation based on measured $\delta^{18}O_w$ normalized to New Delhi.

the nature of the hypsometry within that drainage is not discernable. That analysis is extended here using the recently published compilation of Gajurel et al. (2006) (Fig. 18). Again there is a correlation between observation and prediction, but with a larger degree of scatter than evident in the Rowley and Garzione (2007) analysis. Aspects of this comparison have not been analyzed in detail to determine potential contributions from sampling season or temporal variability of isotopic compositions and their correlations with, for example, know variability recorded at New Delhi, so the significance of the differences are hard to fully assess at this time.

An important point that needs to be emphasized is that the isotopic composition of precipitation is variable on all time scales and so the most robust comparisons should be provided by multi-year, preferably multi-decadal or longer isotopic compositions. The fact that what are essentially instantaneous random grab samples that integrate some uncertain aspect of the hydrography of each of these river systems yield any correlation between isotopic composition and hypsometry is pretty remarkable and provides some confidence in estimates based on archival records that integrate isotopic compositions on a very wide range of time scales (Rowley and Garzione 2007).

The comparison reflected by the data in Figure 18 raises the question-is it possible to measure, for example, the isotopic compositions of bivalve shells, or fish, reptilian or aquatic mammalian teeth preserved within fluvial sediments to determine how high the adjacent mountains were? The implication from Figure 18 is that indeed it should be possible to estimate the precipitation weighted hysometric mean elevation of drainages sampled by such materials. Application of this approach to a paleo-case is presented below.

Figures 19 and 20 present tentative results that show the application of this approach to the Himalayan foreland basin. Soil carbonate-derived oxygen isotopic compositions from

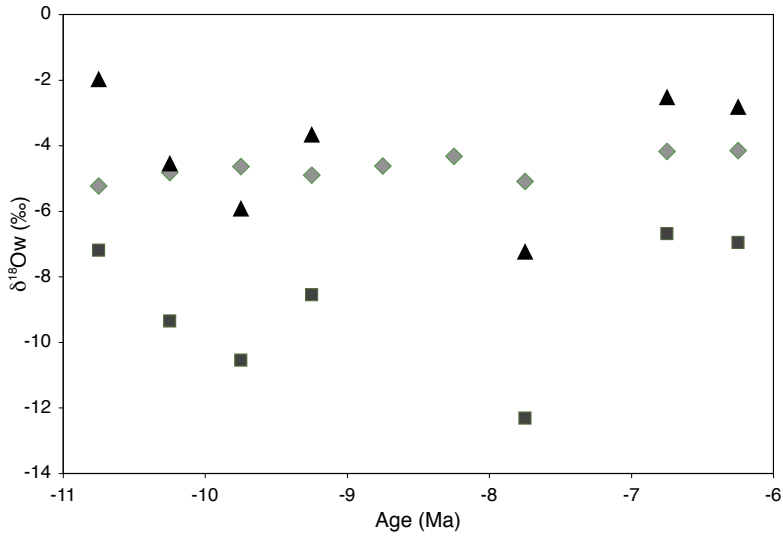

Figure 19. Comparison of Miocene wet season average bivalve isotopic compositions from Dettman et al. (2001) (dark gray squares) with averaged soil carbonate compositions from Bakia Khola (gray diamonds) reported by Harrison et al. (1993) from the Siwaliks. The difference between these is taken as a measure of $\Delta(\delta^{18}O_{mw})$ and hence can be used to estimate the precipitation weighted hypsometric mean elevations of drainages sampled by the bivalve shells. Note that in modern world the wet season amount weighted mean isotopic composition is not significantly from the amount weighted mean annual $\delta^{18}O_p$.

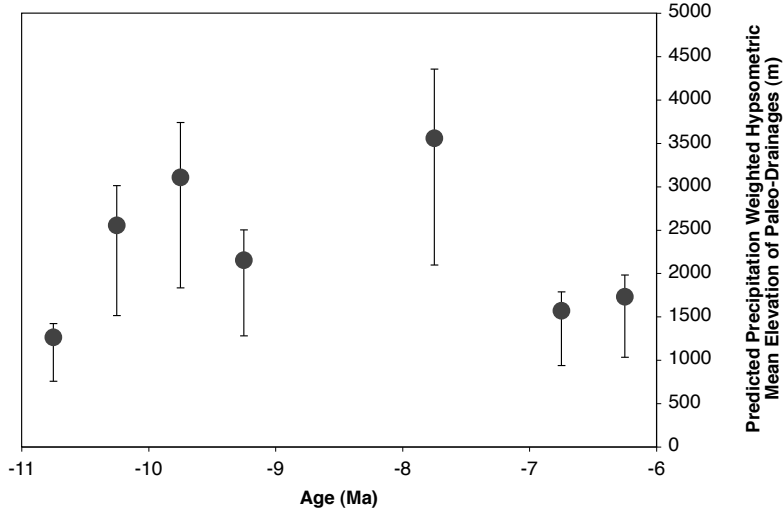

Figure 20. Estimated precipitation weighted hypsometric mean elevations of paleo-drainages sampled by bivalves in the Siwaliks based on estimated $\Delta(\delta^{18}O_{mw})$ shown in Figure 19 as a function of age. Error bars reflect model uncertainty at 2σ based on $\Delta(\delta^{18}O_{mw})$ of the estimated precipitation weighted hypsometric mean elevations.

Bakia Khola reported by Harrison et al. (1993) are used to estimate the isotopic composition of soil waters which are in turn assumed to measure the isotopic composition of low elevation precipitation (Fig. 19). Modern ground waters from the Indo-Gangetic plain are comparable to the weighted mean annual isotopic composition of precipitation measured at New Delhi (Krisnamurthy and Bhattacharya 1991) supporting this assumption. Detailed seasonal isotopic compositions of riverine bivalves preserved within the Siwaliks reported by Dettman et al. (2001) are assumed to provide an estimate of the precipitation weighted hypsometric mean isotopic composition of the drainage basin sampled by a given river system at a given time providing sediments and water to the Siwaliks. The difference between the soil carbonates and bivalve shell compositions are taken as an estimate of $\Delta(\delta^{18}O_{mw})$ that in turn allows an estimate of precipitation weighted hypsometric mean elevation of each of the drainage basins sampled by these bivalves. Note that Figure 19 plots the wet season mean isotopic composition reported by Dettman et al.(2001). In the above discussion of the seasonal variation in isotopic composition of New Delhi it was pointed out that the amount weighted mean monsoon season isotopic composition of precipitation is not significantly different from New Delhi's annual amount weighted mean isotopic composition. Figure 20 implies some temporal variation in z_{pwm} of the drainage basins sampled by these sediments. The variation in time shown on this plot should not be taken to imply changes in Himalayan hypsometry as a whole, but would presumably simply reflect variations in the nature of drainage basin hypsometry being sampled as a function of time. Note also that the paleoelevation estimates are completely compatible with persistence of High Himalayan topography since at least10 Ma (Rowley et al. 1999; Garzione et al. 2000a,b; Rowley et al. 2001) to 20 Ma (France-Lanord et al. 1988; Rowley and Garzione 2007).

CONCLUSIONS

Considerable progress has been made in paleoaltimetry since 1998 when Chase et al. (1998) reviewed the field. The simple 1D thermodynamic model of Rowley et al. (2001) provides a framework for understanding the relationship between stable isotopes and elevation and potential effects of long-term climate change on this relationship. Comparison of transects of precipitation with elevation demonstrate that the model yields good fits to observations, particularly if local temperature and relative humidity conditions are employed (Rowley and Garzione 2007). Existing empirical calibrations are based on temporally limited sampling that may not be representative of the climatological mean conditions, particularly with respect to temperature, to which the modeled relationship is particularly sensitive. Hence their application to the past is uncertain. The global, low latitude, weighted mean model of $\Delta(\delta^{18}O)$ versus elevation represents an ensemble average with variations that, based on comparisons with modern data, appear to robustly capture the characteristic of this relationship. Model based calibrations of $\Delta(\delta^{18}O)$ versus elevation can be computed for any given climatology and hence effects associated with global climate change can be explicitly addressed, which is not possible with empirical calibrations. The model provides a more reasonable estimate of elevation uncertainty than provided by bootstrapping of deviations from limited empirical datasets, since the empirical observations typically capture only a snapshot of climatology that is not likely to be representative of the climatological mean and its variability.

Surface water isotopic compositions do not reflect the local isotopic composition of precipitation, but rather the combined influences of variations in isotopic composition of precipitation as a function of elevation, amount of precipitation as a function of elevation, and drainage basin hypsometry above a given sample elevation. Surface waters thus integrate over the catchment and should be thought of as recording the precipitation amount weighted hypsometric mean elevation of the catchment. Because both the amount of precipitation and typically area decreases with elevation, surface water isotopic compositions are strongly weighted toward recording relatively low elevations. It is difficult to see how to robustly interpret these data in

terms of estimating the full hypsometry of such catchments, and thus deriving estimates of paleoelevations of adjacent mountains from measurement of the isotopic compositions derived from, for example, foreland basin fluvial or lacustrine sedimentary sequences. Evaporation of surface water samples, particularly in lacustrine settings can be significant with the consequent enrichment of the waters, resulting in an underestimate of paleoelevations.

Application of stable isotope-based paleoaltimetry to the Himalayas, Tibet and Andes are beginning to elucidate the evolution of paleotopography in these important orographic systems. These and associated approaches have been applied as well to other regions, including the western Cordillera of North America, Southern Alps of New Zealand and Patagonia. These data are beginning to yield significant insights into the process controlling orogenesis (*sensu stricto*). It is still very early in the development and application of these new techniques, but given the recent progress I look forward to what I suspect will be an increasing number of data sets that will provide insights into the paleoelevation histories of mountain belts. These in turn should provide the basis to test existing ideas and hopefully spur new thinking into the underlying dynamic coupling of tectonics, elevation, surface processes and climate.

ACKNOWLEDGMENTS

First and foremost I want to thank Pratigya Polissar, a Canadian Institute for Advanced Research (CIFAR) Post-Doctoral Fellow shared between Kate Freeman at Pennsylvania State University and myself, for carefully going through the previous version of the model and pointing out several issues with the code. This led to the correction in the computation of the weighted mean curve, and, the reappraisal of the mean elevation at which the condensation is sampled. I also want to thank Matt Kohn for enormous patience as I delayed revisions while recoding and re-validation of these modifications in program. Andreas Mulch, an anonymous reviewer, and particularly Matt Kohn helped clarify the manuscript. This work has been supported by the National Science Foundation through grants EAR-9973222 and EAR-0609782, and the CIFAR-Earth System Evolution Program.

REFERENCES

Ambach W, Dansgaard W, Eisner H, Mooler J (1968) The altitude effect on the isotopic composition of precipitation and glacier ice in the Alps. Tellus 20:595-600

Anders AM, Roe GH, Hallet B, Montgomery DR, Finnegan NJ, Putkonen JK (2006) Spatial Patterns of Precipitation and Topography in the Himalaya. *In*: Tectonics, Climate, and Landscape Evolution, Willet SD, Hovius N, Brandon M, Fisher DM (eds), Geological Society of America, Boulder, CO, p 39-53

Argand E (1924) La Tectonique de L'Asie. Presented at Proceedings of the XIIIth International Geological Congress, Brussels

Bird P (1979) Continental delamination and the Colorado Plateau. J Geophys Res 84:7561-7571

Blisnuik P, Stern L (2005) Stable isotope paleoaltimetry-a critical review. Am J Sci 305:1033-1074

Bowen GJ, Revenaugh J (2003) Interpolating the isotopic composition of modern meteoric precipitation. Water Resour Res 39:9-1–9-13

Burbank DW, Blythe AE, Putkonen J, Pratt-Sitaula B, Gabet E, Oskin M, Barros A, Ojha TP (2003) Decoupling of erosion and precipitation in the Himalayas. Nature 426:652-655

Chamberlain CP, Poage MA (2000) Reconstructing the paleotopography of mountain belts from the isotopic composition of authigenic minerals. Geology 28:115-118

Chase CG, Gregory-Wodzicki KM, Parrish JT, DeCelles PG (1998) Topographic history of the western Cordillera of North America and controls on climate. *In:* Tectonic Boundary Conditions for Climate Reconstruction, Crowley TJ, Burke KC (eds), Oxford University Press, New York, p 73-97

Clark MK, House MA, Royden LH, Whipple KX, Burchfiel BC, Zhang X, Tang W (2005) Late Cenozoic uplift of southeastern Tibet. Geology 33:525-528

Coward MP, Kidd WSF, Pan Y, Shackleton RM, Hu Z (1988) The structure of the 1985 Tibet Geotraverse, Lhasa to Golmud. Phil Trans Roy Soc London 327:307-336

Craig H (1961) Isotopic variations in meteoric waters. Science 133:1702-1708

Currie BS, Rowley DB, Tabor NJ (2005) Middle Miocene paleoaltimetry of southern Tibet: Implications for the role of mantle thickening and delamination in the Himalayan orogen. Geology 33:181-184

Cyr A, Currie BS, Rowley DB (2005) Geochemical and stable isotopic evaluation of Fenghuoshan Group lacustrine carbonates, north-central Tibet:Implications for the paleoaltimetry of Late Eocene Tibetan Plateau. J Geol 113:517-533

Dansgaard W (1964) Stable isotopes in precipitation. Tellus 16:436-468

Dettman DL, Kohn MJ, Quade J, Ryerson FJ, Ojha TP, Hamidullah S (2001) Seasonal stable isotope evidence for a strong Asian monsoon throughout the past 10.7 m.y. Geology 29:31-34

Dewey JF, Shackleton R, Chang CF, Sun YY (1988) The tectonic evolution of Tibet. *In*: The Geological Evolution of Tibet. Phil Trans Roy Soc London 327:379-413

Dutton A, Wilkinson BH, Welker JM, Bowen GJ, Lohman KC (2005) Spatial distribution and seasonal variation in $^{18}O/^{16}O$ of modern precipitation and river water across the conterminous USA. Hydrol Process 19:4121-4146

England P, Housemann G (1986) Finite strain calculations of continental deformation 2. Comparison with the India-Asia collision zone. J Geophys Res 91:3664-3676

France-Lanord C, Sheppard SMF, Le Fort P (1988) Hydrogen and oxygen isotope variations in the High Himalaya peraluminus Manaslu leucogranite: Evidence for heterogeneous sedimentary source. Geochim Cosmochim Acta 52:513-526

Friedman I, Harris JM, Smith GI, Johnson CA (2002a) Stable isotope composition of waters in the Great Basin, United States 1. Air-mass trajectories. J Geophys Res 107:ACL 14-11 - ACL 14-14

Friedman I, Smith GI, Johnson CA, Moscati RJ (2002b) Stable isotope composition of waters in the Great Basin, United States 2. Modern Precipitation. J Geophys Res 107:ACL 15-11 - ACL 15-21

Gajurel AP, France-Lanord C, Huyghe P, Guilmette C, Gurung D (2006) C and O isotope compositions of modern fresh-water mollusc shells and river waters from the Himalaya and Ganga plain. Chem Geol 233:156-183

Garzione CN, Dettman DL, Quade J, DeCelles PG, Butler RF (2000a) High times on the Tibetan Plateau: Paleoelevation of the Thakkhola graben, Nepal. Geology 28:339-342

Garzione CN, Quade J, DeCelles PG, English NB (2000b) Predicting paleoelevation of Tibet and the Himalaya from $\delta^{18}O$ vs. altitude gradients in meteoric water across the Nepal Himalaya. Earth Planet Sci Lett 183:215-229

Garzione CN, Molnar P, Libarkin JC, MacFadden BJ (2006) Rapid late Miocene rise of the Bolivian Altiplano: Evidence for removal of mantle lithosphere. Earth Planet Sci Lett 241:543-556

Garzione CN, Molnar P, Libarkin JC, McFadden BJ (2007) Reply to Comment on "Rapid late Miocene rise of the Bolivian Altiplano:Evidence for removal of mantle lithosphere" by Garzione et al. (2006), Earth Planet Sci Lett 241 (2006) 543–556. Earth Planet Sci Lett 259:630-633

Ghosh P, Garzione CN, Eiler JM (2006) Rapid uplift of the Altiplano revealed through ^{13}C-^{18}O bonds in paleosol carbonates. Science 311:511-515

GLOBE Task Team and others (Hastings DA, Dunbar PK, Elphingstone GM, Bootz M, Murakami H, Maruyama H, Masaharu H, Holland P, Payne J, Bryant NA, Logan TL, Muller J-P, Schreier G, MacDonald JS) (1999) The Global Land One-kilometer Base Elevation (GLOBE) Digital Elevation Model, Version 1.0. National Oceanic and Atmospheric Administration, National Geophysical Data Center. *http://www.ngdc.noaa.gov/mgg/topo/globe.html*

Gonfiantini R, Roche MA, Olivry JC, Fontes JC, Zuppi GM (2001) The altitude effect on the isotopic composition of tropical rains. Chem Geol 181:147-167

Harrison TM, Copeland P, Hall S, Quade J, Burner S, Ojha TP, Kidd WSF (1993) Isotope preservation of Himalayan/Tibetan uplift denudation and climatic histories of two molasse deposits. J Geol 101:157-176

Horita J, Wesolowski DJ (1994) Liquid-vapor fractionation of oxygen and hydrogen isotoopes of water from freezing to the critical temperature. Geochim Cosmochim Acta 58:3425-3437

Horton TW, Chamberlain CP (2006) Stable isotopic evidence for Neogene surface downdrop in the central Basin and Range Province. Geol Soc Amer Bull 118:475-490

Huber M, Caballero R (2003) Eocene El Niño: Evidence for robust tropical dynamics in the "hothouse". Science 299:877-881

Hydro1k (2005) Hydro1k Asia, *http://edc.usgs.gov/products/elevation/gtopo30/hydro/asia.html*

IAEA-Monthly (2004) GNIP2001Monthly.xls, *http://isohis.iaea.org/userupdate\GNIPMonthly.xls*

IAEA-Yearly (2004) GNIP2001Yearly.xls, *http://isohis.iaea.org/userupdate\GNIPYearly2001.xls*

Kalnay E, Kanamitsu M, Kistler R, Collins W, Deaven D, Gandin L, Iredell M, Saha S, White G, Woollen J, Zhu Y, Chelliah M, Ebisuzaki W, Higgins W, Janowiak J, Mo K, Ropelewski C, Wang J, Leetmaa A, Reynolds R, Jenne R, Joseph D (1996) The NCEP/NCAR 40-year reanalysis project. Bull Amer Met Soc 77:437-471

Kent-Corson ML, Sherman LS, Mulch A, Chamberlain CP (2006) Cenozoic topographic and climatic response to changing tectonic boundary conditions in western North America. Earth Planet Sci Lett 252:453-466

Kohn MJ, Miselis JL, Fremd TJ (2002) Oxygen isotope evidence for progressive uplift of the Cascade Range, Oregon. Earth Planet Sci Lett 204:151-165

Kohn MJ, Dettman DL (2007) Paleoaltimetry from stable isotope compositions of fossils. Rev Mineral Geochem 66:119-154

Krisnamurthy RV, Bhattacharya SK (1991) Stable oxygen and hydrogen isotope ratios in shallow ground waters from India and a study of the role of evapotranspiration in the Indian monsoon. *In:* Stable Isotope Geochemistry: A tribute to Samuel Epstein. Taylor HP, O'Neil JR, Kaplan IR (eds), Geochemical Society, San Antonio, Texas, p 187-203

Majoube M (1971a) Fractionnement en 18O entre la glace et la vapeur d'eau. J Chim Phys 68:625-636

Majoube M (1971b) Fractionement en oxygen 18 et en deuterium entre l'eau et sa vapeur. J Chim Phys 68:1423-1436

Merlivat L, Nief G (1967) Isotopic fractionation of solid-vapor and liquid-vapor changes of state of water at temperatures below 0°C. Tellus 19:122-127

Molnar P, England P, Martinod J (1993) Mantle dynamics, uplift of the Tibetan Plateau, and the Indian monsoon. Rev Geophys 31:357-396

Mulch A, Graham SA, Chamberlain CP (2006) Hydrogen isotopes in Eocene river gravels and paleoelevataion of the Sierra Nevada. Science 313:87-89

Mulch A, Chamberlain CP (2007) Stable isotope paleoaltimetry in orogenic belts – the silicate record in surface and crustal geological archives. Rev Mineral Geochem 66:89-118

Poage MA, Chamberlain CP (2001) Empirical relationships between elevation and the stable isotope composition of precipitation and surface waters: Considerations for studies of paleoelevation change. Amer. Jour. Sci. 301:1-15

Putkonen JK (2004) Continuous snow and rain data at 500 to 4400 m altitude near Annapurna, Nepal, 1999–2001. Arctic Antarctic Alpine Res 36:244-248

Pysklywec RN, Beaumont C, Fullsack P (2000) Modeling the behaviour of the continental mantle lithosphere during plate convergence. Geology 28:655-658

Quade J, Garzione C, Eiler J (2007) Paleoelevation reconstruction using pedogenic carbonates. Rev Mineral Geochem 66:53-87

Ramesh R, Sarin MM (1995) Stable isotope study of the Ganga (Ganges) river system. J Hydrol 139:49-62

Roe GH, Montgomery DR, Hallet B (2002) Effects of orographic precipitation variations on the concavity of steady-state river profiles. Geology 30:143-146

Roe GH (2005) Orographic precipitation. Ann Rev Earth Planet Sci 33:645-671

Rowley DB, Pierrehumbert RT, Currie BS, Hosman A, Clayton RN, Hutardo J, Whipple K, Hodges K (1999) Stable isotope-based paleoaltimetry and the elevation history of the High himalaya since the late Miocene. Geol Soc Amer Abstracts with Prog #50213

Rowley DB, Pierrehumbert RT, Currie BS (2001) A new approach to stable isotope-based paleoaltimetry: implications for paleoaltimetry and paleohypsometry of the High Himalaya since the Late Miocene. Earth Planet Sci Lett 188:253-268

Rowley DB, Currie BS (2006) Palaeo-altimetry of the late Eocene to Miocene Lunpola basin, central Tibet. Nature 439:677-681

Rowley DB, Garzione CN (2007) Stable isotope-based paleoaltimetry. Ann Rev Earth Planet Sci 35:463-508

Royden LH, Burchfiel BC, King RW, Wang EC, Chen ZL, Shen F, Liu YP (1997) Surface deformation and lower crustal flow in eastern Tibet. Science 276:788-790

Rozanski K, Araguas-Araguas L, Gonfianti R (1993) Isotopic patterns in modern global precipitation. *In:* Climate Change in Continental Isotopic Records. American Geophysical Union, Washington, p 1-36

Zhu B, Kidd WSF, Rowley DB, Currie BS, Shafique N (2005) Age of initiation of the India-Asia collision in the East-Central Himalaya. J Geol 113:265-285